# Preparation, Structural Characterization, Electrochemistry, and Sensing Properties toward Anions and Cations of Ferrocene–Triazole Derivatives

**ARTICLE** *in* ORGANOMETALLICS · MAY 2013

Impact Factor: 4.13 · DOI: 10.1021/om4002457

ORGANOMETALLICS

Article

pubs.acs.org/Organometallics

# Preparation, Structural Characterization, Electrochemistry, and Sensing Properties toward Anions and Cations of Ferrocene-Triazole Derivatives

Tomás Romero,[†] Raúl A. Orenes,[‡] Alberto Tárraga,*[,†] and Pedro Molina*[,†]

[†]Departamento de Química Orgánica, Facultad de Química, and [‡]Servicio de Apoyo a la Investigación (SAI), Campus de Espinardo, Universidad de Murcia, E-30100 Murcia, Spain

Supporting Information

**ABSTRACT:** A number of monosubstituted (**3**, **4**, **6**, **8**, **9**, **11**, and **13**) and disubstituted (**15** and **16**) ferrocene-derived triazoles have been prepared, by using the copper-catalyzed click reaction, and fully characterized. The versatility of the click reaction enables the decoration of the ferrocene-triazole core, with additional substituents displaying different opto-electrochemical properties. The most salient features derived from the sensing studies are that receptors **3**, **6**, **15**, and **16** undergo unprecedented cathodic shifts of the oxidation peak of the ferrocene/ferrocenium redox couple in the presence of $F^-$, $AcO^-$, $H_2PO_4^-$, and $HP_2O_7^{3-}$ anions, whereas receptors **11** and **16** behave as dual redox and optically selective molecular sensors for $Hg^{2+}$ cations. The isolated $[\mathbf{6}_3{\cdot}Ni^{2+}]$ complex has been characterized by X-ray analysis.

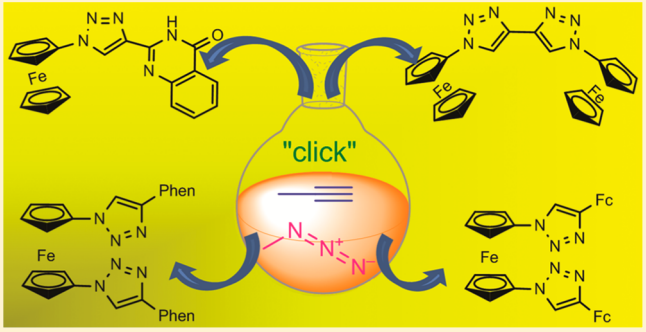


## INTRODUCTION

The independent discoveries of Huisgen's Cu(I)-catalyzed 1,3-dipolar cycloaddition (CuAAC)[1] by Sharpless and Medal[2] have led to thousands of new examples of this reaction subclass. The excellent regioselectivity for the 1,4-isomer of the 1,2,3-triazole and the enhanced reactivity of the Cu(I)-catalyzed process, along with the versatility of the reaction conditions, have made it the flagship reaction of the Sharpless "click" chemistry.[3] As such, it has been widely applied of late, particularly in bioconjugation and drug discovery and also in advanced material sciences toward dendrimers and surface modification.[4] However, much less effort has been devoted to the preparation of organometallic bioconjugates.[5] The 1,2,3-triazole motif has proved to be a versatile ion recognition unit for both cations and anions. As nitrogen-containing Lewis bases, triazole-based ligands have been shown to coordinate transition-metal cations, and accordingly, some triazole-based receptors for the recognition of metals have been reported.[6] In contrast, several triazole derivatives recognize anions through a cooperative triazole C−H···anion hydrogen bond.[7] Several communications making use of a 1,2,3-triazolium cation for phosphate anion recognition, a flexible triazolophane, a triazole-based cyclic peptide, and a preorganized and rigid triazole-based macrocycle, showing self-assembly as well as the anion binding properties of foldamers, all demonstrate 1,2,3-triazoles participating in noncovalent interactions. Interestingly, 1,2,3-triazole-linked dendrimers also showed the ability of binding oxo anions through the 1,2,3-triazole ring localized inside the dendrimers.[8]

It has been recently reported[9] that there are two sources that contribute to the triazole's unexpected anion binding affinity. First, the electronegativities of the three nitrogen atoms combine to polarize the C−H bond. Second, the lone pairs of electron on the nitrogen atoms act to establish and orient along the C−H bond a large 5 D dipole, with its positive end directed almost in line with the C5−H bond. These combined effects make them interesting candidates for amide bond surrogates.[10]

The ferrocene unit has largely proved to be a simple and remarkable redox-signaling unit. Thus, the preparation and sensing properties of ferrocene derivatives have been recently reviewed.[11] In such ferrocene-containing ligands, cation binding at an adjacent receptor site induces a positive shift in the redox potential of the ferrocene/ferrocenium couple by through-space electrostatic communication, and the complexation ability of the ligand can be switched on and off by varying the applied electrochemical potential. The redox-active ferrocene moiety has also been exploited in the electrochemical sensing of anions; these receptors are expected to show cathodic shifts in their redox process on complexation to an anion, as they are easier to oxidize or harder to reduce than a free redox-active receptor. The magnitude of the electrochemical shift ($\Delta E_{1/2}$) upon complexation represents a quantitative measure of the

**Special Issue:** Ferrocene - Beauty and Function

**Received:** March 22, 2013
**Published:** May 20, 2013

**Scheme 1. Preparation of 1-Substituted Ferrocene-Triazoles 3−5, 8, 9, and 11**[a]

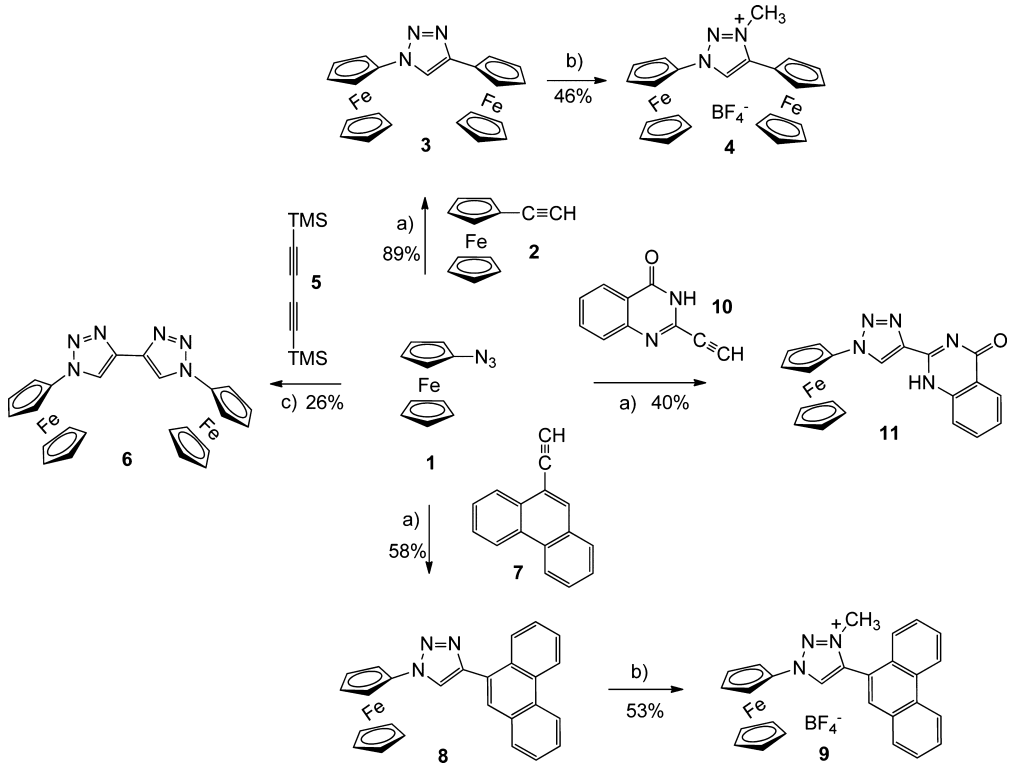


[a]Conditions: (a) $CuSO_4·5H_2O$, sodium ascorbate, $THF/H_2O$, room temperature; (b) $CH_2Cl_2$, $(MeO)_3BF_4$, room temperature; (c) $Bu_4NF$ (TBAF), $CuSO_4·5H_2O$, sodium ascorbate, $THF/H_2O$, rroom temperature.

perturbation of the redox center induced by complexation to the receptor unit.[12]

Ferrocene-triazole derivatives are among the systems that have potential applications in the field of electrochemical detection and sensing and host−guest chemistry.[13]

In this context, we report the synthesis, structural characterization, and electrochemical properties of ferrocene-triazole derivatives in which the triazole ring is additionally linked to a redox unit (ferrocene), a heteroaromatic ring (triazole or quinazolinone), or an aromatic polycyclic ring (phenanthrene). On these bases, suitable dual-signaling chemical probes can be built by combining the redox activity of the ferrocene, the photoactivity of the phenanthrene, and the proven binding ability of the 1,2,3-triazole and quinazolinone rings.

## RESULTS AND DISCUSSION

**Synthesis and Characterization.** The general strategy used for the synthesis of the target ferrocene-triazole derivatives is based on the regioselective CuAAC of terminal alkynes and organic azides and is summarized in Schemes 1−3.

The synthesis of 1-substituted ferrocene-triazoles **3**, **4**, **6**, **8**, **9**, and **11** (Scheme 1) starts with the preparation of azidoferrocene (**1**), by using an improved method consisting of the initial metalation of ferrocene with the system $^t$Bu-Li/$^t$BuOK followed by azidation with trisyl azide (2,4,6-triisopropylbenzenesulfonyl azide).[6p] Compound **1** undergoes the "click" reaction with ethynylferrocene (**2**), 9-ethynylphenanthrene (**7**), and 2-ethynyl-4(3*H*)-quinazolinone[14] (**10**) to afford the triads **3** (89%), **8** (58%), and **11** (40%), respectively, whereas a "click" reaction with 1,4-bis(trimethylsilyl)-1,3-butadiyne (**5**) in the presence of tertrabutylammonium fluoride (TBAF) provides the bisferrocene-bistriazole **6** in 26% yield. Ferrocene-triazolium salts **4** and **9** have been isolated in 46% and 53% yields, respectively, by methylation with trimethyloxonium tetrafluoroborate of the neutral compounds **3** and **8**. Copper(I) and oxidized copper(II) species in the reaction mixture can be easily separated by treatment with aqueous ammonia during the workup and subsequent crystallization.

Preparation of the 4-substituted ferrocene-triazole **13** involves the previous synthesis of the 1-pyrenyl azide **12**, following a previously reported procedure.[15] Thus, 1-pyrenyl azide **12** reacted with ethynylferrocene **2** under the same reaction conditions to afford the 4-ferrocenyl-substituted triazole **13** in 59% yield (Scheme 2).

**Scheme 2. Preparation of 1,1′-Disubstituted Ferrocene-Triazole 13**[a]

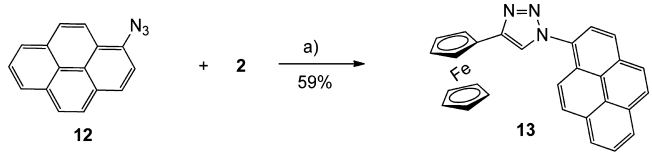


[a]Conditions: (a) $CuSO_4·5H_2O$, sodium ascorbate, $THF/H_2O$, room temperature.

The synthesis of the 1,1′-disubstituted ferrocene-triazoles **15** and **16** (Scheme 3) requires the use of previously prepared 1,1′-bis(azido)ferrocene **14** by a two-step sequence: bislithiation of ferrocene and subsequent treatment with the aforementioned strong azide-transfer agent trisyl azide.[16] A subsequent "click" reaction of compound **14** with ethynyl derivatives **2** and **7** affords the 1,1′-disubstituted ferrocene-


dx.doi.org/10.1021/om4002457 | *Organometallics* 2013, 32, 5740−5753

**Scheme 3. Preparation of 1,1′-Disubstituted Ferrocene-Triazoles 15 and 16**[a]

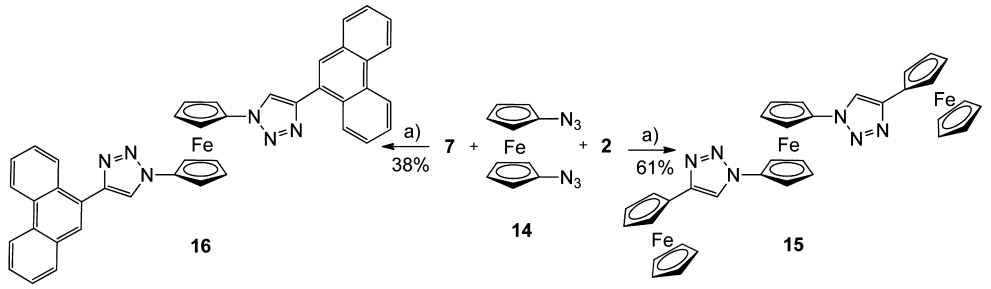


[a]Conditions: (a) $CuSO_4·5H_2O$, sodium ascorbate, $THF/H_2O$, room temperature.

triazoles **15** and **16** in 61% and 38% yields, respectively (Scheme 3).

The structures of all the synthesized compounds were elucidated using extensive spectral studies ($^1$H NMR, 2D COSY, 2D NOESY, $^{13}$C NMR, and HMQC spectra, as well as electrospray mass spectra (ESI-MS)) and elemental analysis.

The $^1$H NMR spectra of the neutral compounds display one singlet at $\delta$ values ranging from 7.63 ppm in **15** to 8.55 ppm in **11**, corresponding to the triazole ring proton. Moreover, the nonequivalence of the *N*-ferrocenyl (N-Fc) and *C*-ferrocenyl (C-Fc) units attached to the triazole ring present in these receptors is clearly evidenced through the inspection of both the $^1$H and $^{13}$C NMR spectra. Thus, a characteristic feature of these $^1$H NMR spectra is the appearance of a pair of well-defined pseudotriplets, corresponding to the $H_\alpha$ and $H_\beta$ protons of their monosubstituted Cp moieties and one singlet, for the five protons within the unsubstituted Cp moieties. In order to further discriminate between the set of signals associated to the N-Fc and C-Fc units present in compounds **3**, **4**, **13**, and **15** $^1$H−$^1$H-COSY and NOESY spectra were carried out (see the Experimental Section and Supporting Information). A general characteristic feature is the appearance of the $H_\alpha$ pseudotriplets, of both N-Fc and C-Fc units, at downfield with reference to the signals corresponding to the $H_\beta$ protons (Table S1 in the Supporting Information). Figure 1

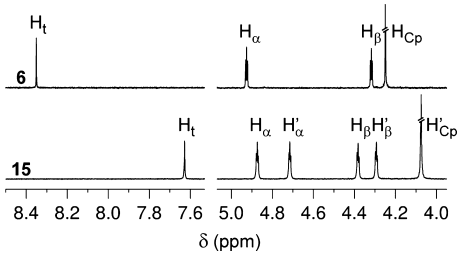


**Figure 1.** Comparison between the $^1$H NMR spectrum of 1,1′-diferrocenyl-1*H*,1′*H*-4,4′-bi(1,2,3-triazole) (**6**), containing only N-Fc units, and 1,1′-bis[(4-ferrocenyl)-1*H*-1,2,3-triazol-1-yl]ferrocene (**15**), bearing both N-Fc ($H_\alpha$, $H_\beta$, $H_{Cp}$) and C-Fc ($H'_\alpha$, $H'_\beta$, $H'_{Cp}$) units.

represents a clear example of the aforementioned general characteristic spectral features. Thus, the $^1$H NMR spectrum of **6** shows a singlet at $\delta$ 4.25 ppm corresponding to the unsubstituted Cp ring protons of the N-Fc unit, while those present in the monosubstituted Cp ring appear as two pseudotriplets located downfield at $\delta$ 4.93 ppm for the $H_\alpha$ protons and at $\delta$ 4.32 ppm for the $H_\beta$ protons. The $^1$H NMR spectrum of **15** exhibits the characteristic two peudotriplets at $\delta$ 4.87 and 4.38 ppm for the two pairs of nonequivalent $H_\alpha$ and $H_\beta$ protons present in the 1,1′-disubstituted N-Fc moiety, together with another two signals at $\delta$ 4.72 and 4.29 ppm for the $H_\alpha$ and $H_\beta$ protons present in the monosubstituted Cp ring of the C-Fc unit. In this case, the signal belonging to the unsubstituted Cp ring of the N-Fc appears as a singlet integrating for 10 protons at $\delta$ 4.07 ppm.

Taking a closer look at the $^1$H NMR of compounds **6** and **15**, a significant deshielding ($\Delta\delta$ = 0.70 ppm) for the triazole CH proton in **6** ($\delta$ 8.35 ppm) with reference to **15** ($\delta$ 7.65 ppm) is observed, which could be attributed to the formation of an intramolecular hydrogen bond between this CH proton and the N3 atom belonging to the adjacent triazole ring. A similar effect could also be responsible for the chemical shift observed for the triazole CH proton in receptor **11** ($\delta$ 8.55 ppm), where a similar hydrogen bond between the triazole CH proton and the nitrogen atom within the quinazolinone ring could also take place.

Due to the excellent mobility around the organometallic bond, the 1,1′-disubstituted ferrocene derivative **16** could exist as *syn* and *anti* conformers, which could be interconverted as a consequence of the well-known low rotational barrier around the organometallic bond showed by the ferrocene spacer group. This rotation has been studied in 1,1′-diaryl- and 1,1′-di(azaheteroaryl)-substituted ferrocenes,[17] and an examination of the NMR data revealed that aryl and azaheteroaryl protons of the disubstituted derivatives showed larger upfield shifts with reference to the analogous protons present in the corresponding monosubstituted derivative. In those cases, the shielding effects were reported to be a consequence of a $\pi$ stacking of the aromatic or heteroaromatic rings present in both arms of the ferrocene moiety. In this context, we have also found that protons of the disubstituted ferrocene **16** are shielded and hence shifted upfield in comparison with the analogous resonances of the monosubstituted derivative **8** (Figure 2).

It is also worth mentioning that in all the cases the ESI-MS shows the corresponding $[M^+ + 1]$ peaks, in agreement with the proposed structures.

**X-ray Structural Characterization.** Single-crystal X-ray diffraction was also used to confirm the molecular structure of the neutral 1,2,3-triazole derivatives **8**, **11**, and **13** (Table S2 (Supporting Information)) as well as the ferrocenyl 1,2,3-triazoliums **4** and **9** (Table S3 (Supporting Information)).

X-ray-quality single crystals of **8** were grown from $CH_2Cl_2$; it crystallizes as an orange prism in the monoclinic space group $P2_1$. The Cp rings are arranged in an almost eclipsed conformation (the average torsion angle C1′−centroid (Cp)1−centroid (Cp)2−C6′ is 4.58°) and have an almost parallel orientation with a tilt angle of 1.7°. The triazole ring attached to the C1′ atom is rotated with respect to the C1′-Cp


dx.doi.org/10.1021/om4002457 | *Organometallics* 2013, 32, 5740−5753

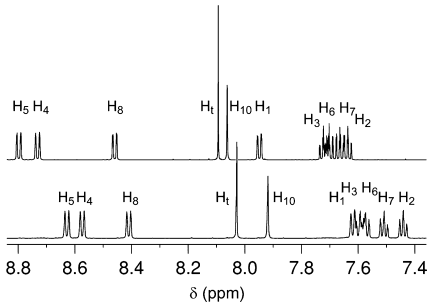


**Figure 2.** Aromatic region of the $^1$H NMR spectrum ($CDCl_3$, 600 MHz) of receptors **8** (top) and **16** (bottom). $H_t$ corresponds to the signal of the triazole proton, and $H_1$–$H_{10}$ indicate the protons within the phenanthrene ring.

ring, the angle between mean planes being 19.6°. The phenanthrene moiety is rotated with respect to the triazole by 143.7° and with respect to the C1′-Cp ring by 157.0° (Figure 3a and Tables S4–S7 (Supporting Information)). In the crystal, molecules are displayed in two different orientations related by an angle of 58.3° between their phenanthrene rings. Molecules with the same orientation are stacked along the *c* axis, the phenanthrene moiety of the molecules interacting via *π*–*π* stacking. The mean planes of the staked rings are separated by 3.46 Å with a parallel displacement of 5 Å aproximately in a way that the overlapping is only partial, the C1-ring of the phenanthrene of one molecule interacting with the C8-ring of the phenanthrene of other molecule situated in an upper plane (Figures S44–S46 (Supporting Information)).

Compound **11** crystallizes from acetonitrile as a yellow prism in the monoclinic space group $P2_1/n$. The Cp rings are arranged in an almost eclipsed conformation (the average torsion angle C1–centroid (Cp)1–centroid (Cp)2–C6 is 7.78°) and have an almost parallel orientation with a tilt angle of 1.2°. The organic moiety attached to the C1 atom is nearly planar, the mean deviation from planarity being 0.0694 Å, and is rotated by 44.2° with respect to the C1-Cp ring. The triazole is rotated with respect to the C1-Cp ring by 35.6° and the fused ring is rotated with respect to the triazole by 12.1° and with respect to the C1-Cp ring by 46.3° (Figure 3b and Tables S8–S12 (Supporting Information)). In the crystal structure, molecules are interlinked by four intermolecular hydrogen bonds (C11–H11···O1 and N4–H04···O1) forming dimers (Figure S47 (Supporting Information)). In the dimer, molecules are related by an inversion center. These dimers are linked to others by intermolecular C8–H8···N5 hydrogen bonds, producing a 3D lattice.

Compound **13** crystallizes from dichloromethane/pentane as an orange prism in the monoclinic space group $P2_1$ (Figure 3c and Tables S13–S17 (Supporting Information)). The Cp rings are arranged in an almost eclipsed conformation (the average torsion angle C1–centroid (Cp)1–centroid (Cp)2–C6 is 10.25°) and have a parallel orientation with a tilt angle of 0.8°. The triazole ring attached to the C1 atom is almost parallel to the C1-Cp ring, the angle between mean planes being 4.2°. The fused ring attached to the triazole is planar (the mean deviation from plane being 0.017 Å) and rotated with respect to the triazole by 57.9° and with respect to the C1-Cp ring by 62.1°. In the crystal, molecules are interlinked by intermolecular C12–H12···N2 hydrogen bonds forming single chains along the *c* axis. In the chains, molecules also display C35H35–*π* interactions, the distance between H35 and the

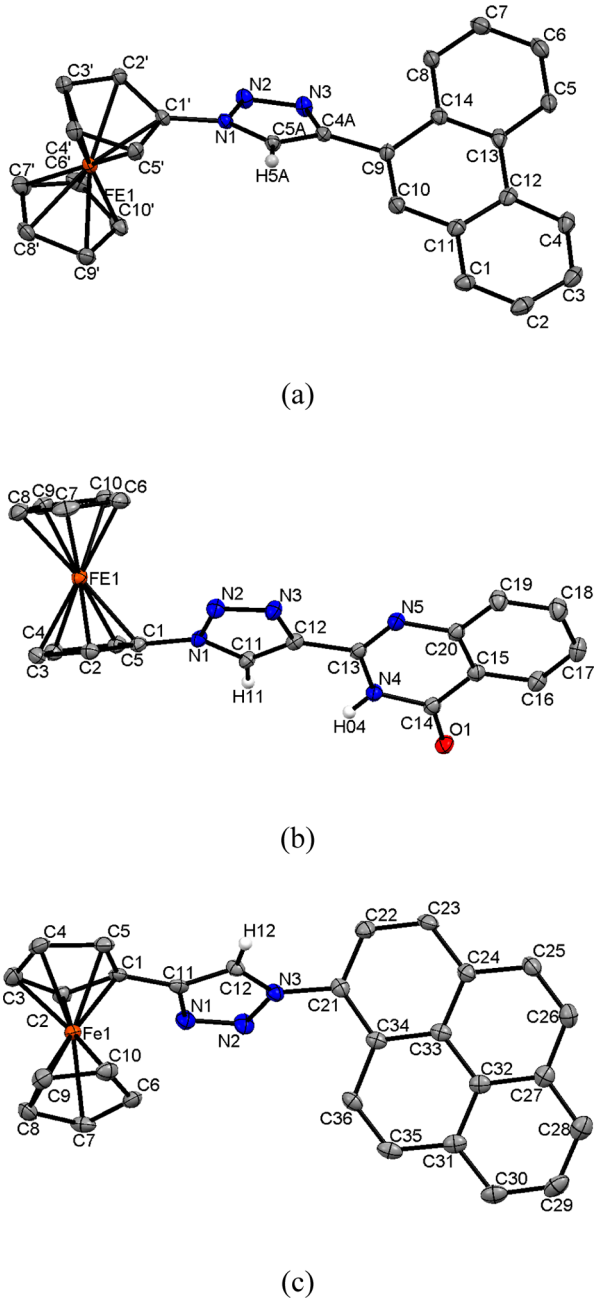


**Figure 3.** ORTEP drawings for the ferrocenyl-triazole derivatives **8** (a), **11** (b), and **13** (c) with the numbering scheme. Thermal ellipsoids are drawn at 50% probability level. Selected bond lengths (Å) and angles (deg): for **8**, N(1)–C(1′) = 1.424(2), C(4A)–C(9) = 1.483(2), N(2)–N(1)–C(1′) = 120.52(13), C(5A)–N(1)–C(1′) = 128.49(14), N(3)–C(4A)–C(9) = 124.65(14), C(5A)–C(4A)–C(9) = 127.55(15); for **11**, N(1)–C(1) = 1.422(2), C(12)–C(13) = 1.465(2), C(11)–N(1)–C(1) = 128.19(14), N(2)–N(1)–C(1) = 121.29(13), N(3)–C(12)–C(13) = 121.24(15), C(11)–C(12)–C(13) = 130.30(15); for **13**, N(3)–C(21) = 1.433(3), C(1)–C(11) = 1.461(3), C(12)–N(3)–C(21) = 126.6(2), N(2)–N(3)–C(21) = 122.5(2), N(1)–C(11)–C(1) = 121.5(2), C(12)–C(11)–C(1) = 130.2(2).

centroid of the fused ring being 3.027 Å. These interactions may be responsible for the angle formed between the triazole and the fused ring (Figure S48 (Supporting Information)).

Crystals suitable for single-crystal X-ray analysis were also obtained for the 1,2,3-triazolium receptors **4** and **9**. Compound


dx.doi.org/10.1021/om4002457 | *Organometallics* 2013, 32, 5740–5753

4 crystallizes from chloroform/hexane as an orange lath in the monoclinic space group $P2_1/c$ (Figure 4a and Tables S18−S22

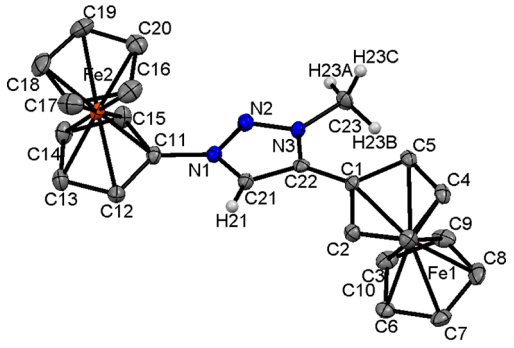


(a)

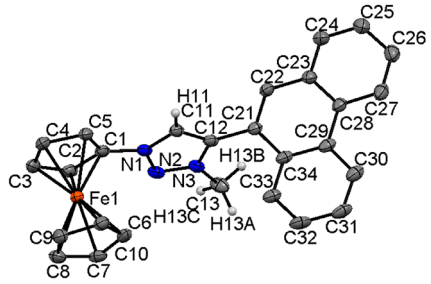


(b)

**Figure 4.** ORTEP drawings for the ferrocenyl-triazolium derivatives **4** (a) and **9** (b) with the numbering scheme. Thermal ellipsoids are drawn at the 50% and at 35% probability levels for **4** and **9**, respectively. Selected bond lengths (Å) and angles (deg): for **4**, N(1)−C(11) = 1.423(3), C(22)−C(1) = 1.449(3), N(2)−N(1)−C(11) = 119.23(16), C(21)−N(1)−C(11) = 127.86(17), N(3)−C(22)−C(1) = 126.87(18), C(21)−C(22)−C(1) = 128.60(18); for **9**, N(1)−C(1) = 1.424(4), C(12)−C(21) = 1.476(4), N(2)−N(1)−C(1) = 119.3(2), C(11)−N(1)−C(1) = 128.6(3), C(11)−C(12)−C(21) = 132.1(3), N(3)−C(12)−C(21) = 123.6(3).

(Supporting Information)). The asymmetric unit consists of one cation and one tetrafluoroborate anion. The ferrocenyl moieties of the cation are orientated in an *anti* conformation and bridged by a triazole ring. The C22 atom of the triazole is attached to the C1 of a ferrocenyl unit (C-Fc) and its N2 atom to the C11 of another ferrocenyl moiety (N-Fc). The Cp rings of the C-Fc are arranged in an eclipsed conformation (the average torsion angle C1−centroid (Cp)1−centroid (Cp)2−C10 is 1.43°) and have an almost parallel orientation with a tilt angle of 1.6°. The Cp rings of the N-Fc are twisted from the eclipsed conformation (the average torsion angle C11−centroid (Cp)3−-centroid (Cp)4−C20 being 33.02°) and parallel oriented (tilt angle of 0.8°). The triazole is rotated by 18.1° with respect to the C1-Cp ring and 12.2° with respect to the C11-Cp ring and the C1-Cp ring is rotated by 10.4° with respect to the C11-Cp ring.

In the crystal structure, molecules present two different orientations, the triazole mean planes of these molecules BEING related by a rotation of 67.16°. Molecules with the same orientation are interlinked using the tetrafluoroborate anions as bridges via four intermolecular hydrogen bonds (C23−H23A···F4, C10−H10···F3, C16−H16···F4, and C21−H21···F2) forming ribbons along the *c* axis (Figure 5). These ribbons are linked to tetrafluoroborate anions through the hydrogen-bonding pattern C23−H23C···F1···H6−C6 along the *b* axis, producing a 3D network.

Compound **9** crystallizes from chloroform as an orange prism in the monoclinic space group $P2_1/n$ (Figure 4b and Tables S23−S27 (Supporting Information)). The Cp rings are arranged in an almost eclipsed conformation (the average torsion angle C1−centroid (Cp)1−centroid (Cp)2−C6 is 9.17°) and have an almost parallel orientation with a tilt angle of 2.7°. The triazole ring attached to the C1 atom is nearly parallel to the C1-Cp ring, the angle between mean planes being 7.8°. The phenanthrene moiety is perpendicular to the C1-Cp ring (angle between mean planes 93.5°) and is rotated with respect to the triazole by 101.2°. In the crystal, molecules are displayed in two different orientations related by an angle of 66.5° between their phenanthrene rings. Molecules with the same orientation stack perpendicular to the *a* axis, forming dimers, the phenanthrene moiety of the molecules interacting via $\pi-\pi$ stacking. In the dimers, the mean planes of the phenanthrene rings are separated by 3.55 Å and show a parallel displacement of 1.5 Å approximately in a way that the overlapping is only partial. Four molecules of tetrafluoroborate acting as bridges keep the molecules of the dimers close together via hydrogen bonds (C3−H3···F2, C13−H13A···F4, and C30−H30···F3···H11−C11) along the *c* axis. Each tetrafluoroborate anion interacts with four different molecules: molecules 1 and 2 present the same orientation and form a dimer, and molecules 3 and 4 are displayed in the other orientation, and each of them forms a dimer with another molecule. The result is a complex network of hydrogen bonds producing a 3D lattice (Figures S49−S52 (Supporting Information)).

**Electrochemical and Optical Properties.** The redox chemistry of all the triazole and triazolium derivatives synthesized has been investigated by CV and OSWV in $CH_3CN$ solutions containing 0.1 M TBAHP as supporting electrolyte. Mono- and bis-triazole receptors bearing one *N*-ferrocene moiety exhibited in the range 0−1.0 V a reversible one-electron redox wave, typical of a ferrocene derivative, at a half-wave potential ranging from $E_{1/2}$ = 709 mV to $E_{1/2}$ = 871 mV versus decamethylferrocene (DMFc). In contrast, compound **13** bearing a *C*-ferrocene unit shows the corresponding reversible one-electron oxidation wave at $E_{1/2}$ = 565 mV (Table S28 (Supporting Information)). On the other hand, the neutral receptors **3** and **15** showed two different and reversible one-oxidation waves at $E_{1/2}$ = 560 mV (C-Fc) and $E_{1/2}$ = 749 mV (N-Fc), in the case of **3**, and $E_{1/2}$ = 544 mV (C-Fc) and $E_{1/2}$ = 953 mV (N-Fc), in the case of **15**. From these data is clear that the oxidation potentials of the ferrocenyl units are strongly dependent on the position of the triazole bridge to which they are attached, the oxidation being easier when the ferrocene is linked to the 4-position of the heterocyclic ring (C-Fc) ($E_{1/2}$ around 500 mV) than when it is linked to the 1-position (N-Fc) ($E_{1/2}$ around 700 mV). The positively charged triazolium derivatives **4** and **9** displayed electrochemical responses similar to those of their neutral precursors, although the corresponding oxidation waves appeared at more positive potentials as a consequence of the cationic nature of these receptors: $E_{1/2}$ = 835 mV (C-Fc) and $E_{1/2}$ = 907 mV (N-Fc), in the case of **4**, and $E_{1/2}$ = 901 mV (N-Fc), in the case of **9**.[18] Likewise, the


dx.doi.org/10.1021/om4002457 | *Organometallics* 2013, 32, 5740−5753

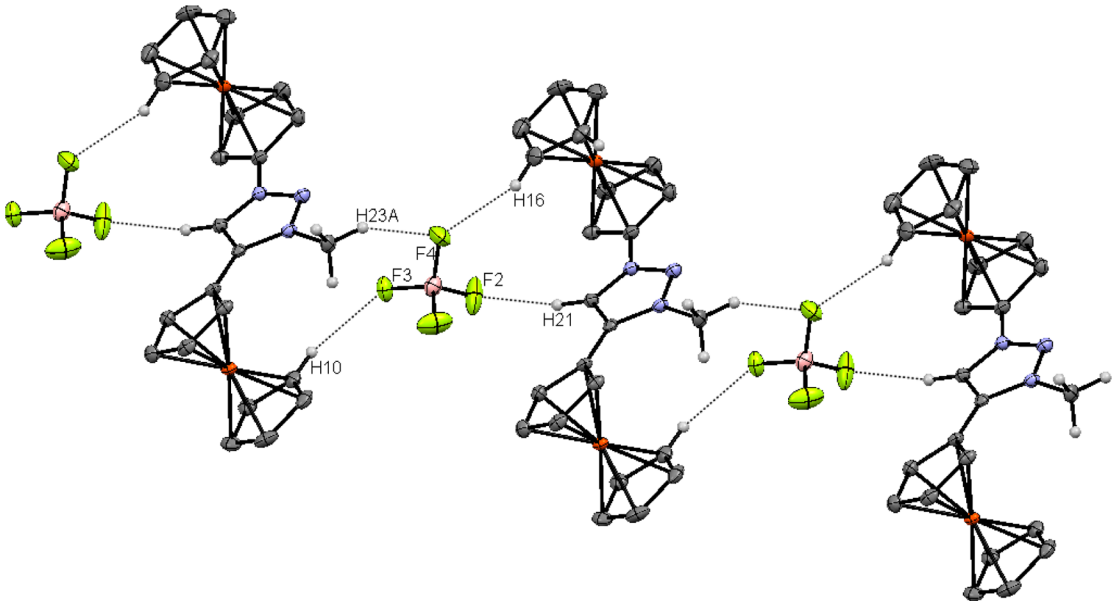


**Figure 5.** Ribbon formation in the crystal structure of **4**. Some hydrogen atoms have been omitted for clarity.

OSWV obtained for all the ferrocene-triazole species prepared also exhibits oxidation peaks at the same potentials observed in the corresponding CV.

The UV−visible data obtained for these receptors are consistent with most ferrocenyl chromophores in that they exhibit two charge-transfer bands in the UV−visible region.[19] These spectra contain an absorption band with a maximum at around 320 nm which can safely be ascribed to a high-energy ligand-centered $\pi-\pi^*$ electronic transition (L-$\pi^*$) (HE band). In addition to this band, another weaker absorption is visible at around 450 nm, which is assigned to another localized excitation with a lower energy produced by two nearly degenerate transitions, by a Fe(II) d−d transition,[20] or by a metal−ligand charge transfer (MLCT) process ($d_\pi-\pi^*$) (LE band). This assignment is in accordance with the latest theoretical treatment (model III) reported by Barlow et al.[21] Such spectral characteristics confer a yellow color to these species. On the other hand, in the ferrocene derivatives **4** and **9**, bearing one triazolium unit, these two charge-transfer bands are red-shifted with reference to those appearing in the corresponding neutral precursors and are responsible for the orange color of such species (Figure 6).

The emissive properties of receptors **8**, **9**, **13**, and **16**, bearing a photoactive phenanthrene or pyrene group connected to the ferrocene moiety by the 1,2,3-triazole ring, have also been studied. However, the combination of these two structural elements, ferrocene and triazole ring, promote a fluorescent quenching effect induced, possibly, by a photoinduced electron transfer (PET) process.[22] Consequently, these receptors exhibit a very weak emission spectra in $CH_3CN$ ($c = 1 \times 10^{-5}$ M) when excited at the appropriate $\lambda_{exc}$, with rather low quantum yields:[23] $\Phi = 4 \times 10^{-4}$ for **8**, $\Phi = 4 \times 10^{-3}$ for **9**, $\Phi = 2 \times 10^{-3}$ for **13**, and $\Phi = 1 \times 10^{-3}$ for **16**.

**Ion Binding Studies.** *Electrochemical Recognition.* Chemical receptors bearing redox-active ferrocene moieties as sensing units have been broadly studied to recognize and sense not only metal cations[11] but also anionic species.[24] Moreover, the direct linkage of this redox-active unit to a 1,2,3-triazole ring, containing two quite different binding sites such as $sp^2$-hybridized N atoms, able to bind metal cations, and a CH, able to promote CH···anion interactions, allows the evaluation of the chemosensing properties of these ligands by electrochemical techniques.

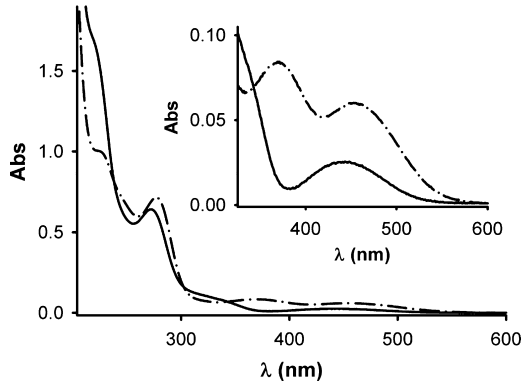


**Figure 6.** Absorption spectra of **3** (solid line) and **4** (dash-dotted line) in $CH_3CN$ ($c = 5 \times 10^{-5}$ M). The inset shows the main differences observed in the 300−600 nm region of the UV−vis spectra of both receptors.

Thus, their electrochemical behavior in the presence of several anions ($F^-$, $Cl^-$, $Br^-$, $AcO^-$, $NO_3^-$, $HSO_4^-$, $H_2PO_4^-$, and $HP_2O_7^{3-}$), added as tetrabutylammonium salts ($TBA^+$), and metal cations ($Li^+$, $Na^+$, $K^+$, $Mg^{2+}$, $Ca^{2+}$, $Ni^{2+}$, $Cu^{2+}$, $Zn^{2+}$, $Cd^{2+}$, $Hg^{2+}$, and $Pb^{2+}$), as their perchlorate or triflate salts,[25] was investigated by linear sweep voltammetry (LSV), CV, and OSWV.[26]

Titration studies with addition of anions to an electrochemical solution of the neutral receptors **3**, **6**, **11**, **15**, and **16** ($c = 10^{-4}$ M) in $CH_3CN$ (**3**, **11**, and **16**) or $CH_3CN/CH_2Cl_2$ (1/1) (**6** and **15**) containing TBAHP (0.1 M) as supporting electrolyte, demonstrate that while addition of $F^-$, $AcO^-$, $H_2PO_4^-$, and $HP_2O_7^{3-}$ anions promotes remarkable responses, addition of $Cl^-$, $Br^-$, $NO_3^-$, and $HSO_4^-$ had no effect on either the CV or OSWV of these receptors, even when present in a large excess. The results obtained on the stepwise addition of increasing amounts of the appropriate guest anionic species revealed a typical "shifting behavior" in which a second redox


dx.doi.org/10.1021/om4002457 | *Organometallics* 2013, 32, 5740−5753

wave, associated with the formation of a complexed species and negatively shifted in comparison to the free receptor, appears.[27] The current intensity of this new peak increases until 10 equiv of the guest anion is added. At this point, the peak corresponding to the uncomplexed receptor disappears. Interestingly, the anion coordination involves a different effect on the oxidation potential of both types of ferrocene units present in these receptors. Thus, a more pronounced negative shifting effect is observed for the oxidation potential of the N-Fc units in comparison to that for the C-Fc, as it is easily demonstrated in the cases of receptors **3** ($\Delta E_{1/2}$ = −80 mV for $F^-$, $\Delta E_{1/2}$ = −221 mV for $AcO^-$, $\Delta E_{1/2}$ = −217 mV for $H_2PO_4^-$, and $\Delta E_{1/2}$ = −259 mV for $HP_2O_7^{3-}$) (Figure 7 and

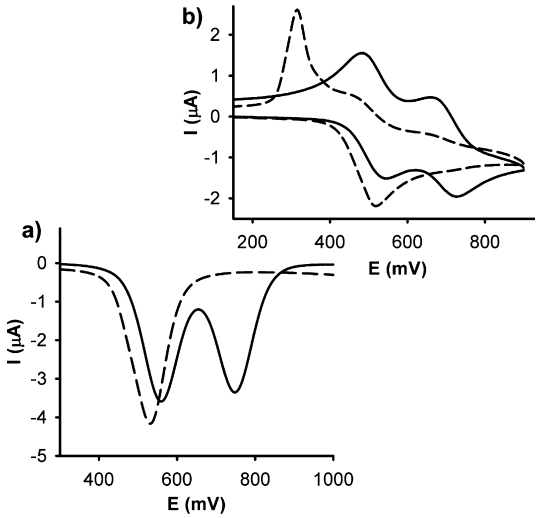


**Figure 7.** Evolution of the (a) OSWV and (b) CV of ($c = 1 \times 10^{-4}$ M) **3** in $CH_3CN$/*n*-$Bu_4NPF_6$ scanned at 0.1 V $s^{-1}$ (solid lines) and scanned upon addition of $H_2PO_4^-$ (dashed lines).

Table S28 and Figures S53−S56 (Supporting Information)) and **15** ($\Delta E_{1/2}$ = −245 mV for $F^-$, $\Delta E_{1/2}$ = −100 mV for $AcO^-$, $\Delta E_{1/2}$ = −345 mV for $H_2PO_4^-$, and $\Delta E_{1/2}$ = −333 mV for $HP_2O_7^{3-}$) (Table S28 and Figures S58−S61 (Supporting Information)), whereas lower values of the cathodic shifts were observed for receptors **6** and **16**. Interestingly, both types of ferrocene units present in the complexes formed by **3** with the corresponding anions undergo oxidation at the same potential, except in the case of the $F^-$ anion, in which the N-Fc and C-Fc oxidation peaks are shifted by $\Delta E_{1/2}$ = −80 mV and $\Delta E_{1/2}$ = −40 mV, respectively. The cathodic shifts observed can be explained in such a way that the electron density in anions is transferred to the ferrocenyl moieties which, as a consequence, are oxidized more easily to the corresponding ferrocenium ions.

To verify whether the perturbations observed upon addition of $F^-$, $AcO^-$, $H_2PO_4^-$, and $HP_2O_7^{3-}$ anions to the free receptor **11**, bearing a NH group, were associated with a recognition event, involving the formation of a hydrogen-bonded complex between **11** and such anions, or to a deprotonation process of such a free ligand, we carried out other electrochemical experiments by aeither dding $Bu_4NOH$ to the electrochemical solution of the free receptor, which definitely lead to deprotonation, or titrating with these anions in the presence of acetic acid, in which case the deprotonation process is prevented.[28] First, titration with the strong base $Bu_4NOH$ gave rise to the appearance of a new oxidation peak, cathodically shifted by $\Delta E_{1/2}$ = −140 mV. This magnitude is quite similar to that obtained for the cathodic shift of the oxidation peak resulting upon addition of those anions ($\Delta E_{1/2}$ around −150 mV in all cases). Second, titrations with such anions in the presence of 20 equiv of AcOH gave rise to the same electrochemical response as that observed for the free receptor. These data clearly suggest that the perturbations observed upon addition of $F^-$, $AcO^-$, $H_2PO_4^-$, and $HP_2O_7^{3-}$ anions to the free receptor **11** should be associated with a deprotonation event.

The anion-binding properties of the triazolium quaternary salts **4** and **9**, in which the C-5 proton of the triazolium ring actively participates in the recognition of anions through C−H···$A^-$ hydrogen bond interactions,[29] have also been studied. Thus, their electrochemical behavior was investigated in the presence of the same set of anions tested for the neutral receptors and under the same electrochemical conditions. However, the strongly increased C(5)H acidity in the 1,2,3-triazolium systems, in comparison to the 1,2,3-triazole precursors, gave rise to a slight loss of selectivity in the recognition process. As a consequence, titration experiments with addition of $F^-$, $Cl^-$, $Br^-$, $AcO^-$, $NO_3^-$, $HSO_4^-$, $H_2PO_4^-$, and $HP_2O_7^{3-}$ anions revealed that receptor **4** shows remarkable cathodic shifts upon addition of $F^-$ ($\Delta E_{1/2}$ = −232 mV), $Cl^-$ ($\Delta E_{1/2}$ = −106 mV), $Br^-$ ($\Delta E_{1/2}$ = −161 mV), $AcO^-$ ($\Delta E_{1/2}$ = −221 mV), $H_2PO_4^-$ ($\Delta E_{1/2}$ = −381 mV), and $HP_2O_7^{3-}$ anions ($\Delta E_{1/2}$ = −387 mV). Meanwhile, receptor **9** undergoes redox perturbation to a lesser extent in the presence of $F^-$, $AcO^-$, $H_2PO_4^-$, and $HP_2O_7^{3-}$ (Figure 8 and Table S28 and Figures S62−S65 (Supporting Information)).

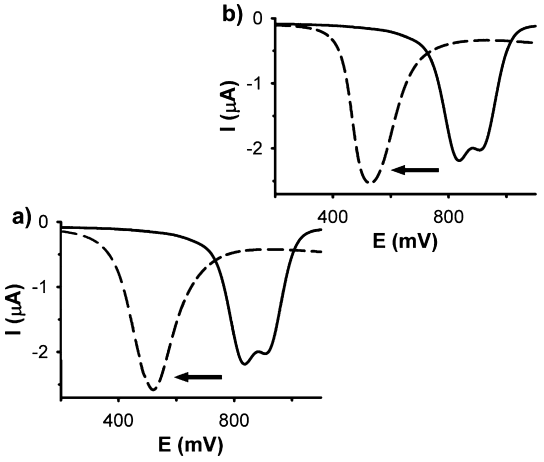


**Figure 8.** Evolution of the OSWV of **4** in $CH_3CN$ ($c = 1 \times 10^{-4}$ M)/*n*-$Bu_4NPF_6$ scanned at 0.1 V $s^{-1}$ (solid lines) in the presence of (a) $HP_2O_7^{3-}$ and (b) $H_2PO_4^-$ anions (dashed lines).

We have also studied the role of the 1,2,3-triazole moiety as an cation-sensing moiety; no significant changes occurred in the CV or OSWV of the monotriazole derivatives **3**, **8**, and **13** upon addition of any of the metal cations tested, even when present in a large excess. However, the behaviors of the monotriazole **11**, with a quinazolinone ring appended to the C4 of the triazole ring, as well as the bistriazole derivatives **6**, **15**, and **16** are completely different. Thus, for **11**, only the stepwise addition of $Hg^{2+}$ resulted in the appearance of a new oxidation peak at a more positive potential ($E_{1/2}$ = 824 mV, $\Delta E_{1/2}$ = +72 mV), indicating the formation of the corresponding complex (Figure 9a). With reference to the electrochemical titration studies carried out by using the symmetrical bistriazole **6**, only the addition of $Ni^{2+}$, $Hg^{2+}$, and $Pb^{2+}$ induced the appearance, in


dx.doi.org/10.1021/om4002457 | *Organometallics* 2013, 32, 5740−5753

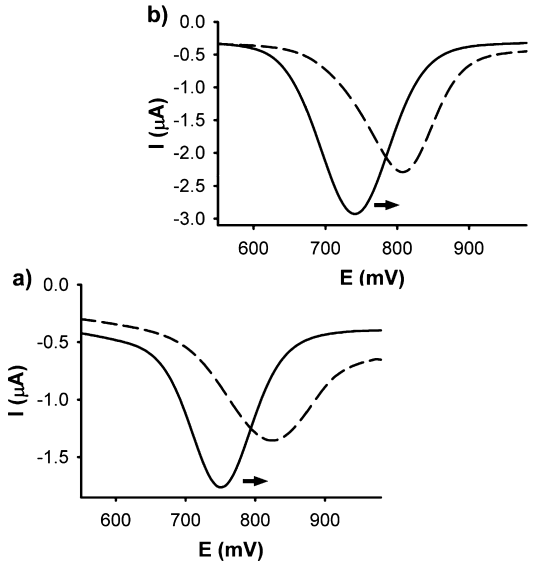


**Figure 9.** (a) Evolution of the OSWV of **11** ($c = 1 \times 10^{-4}$ M) in $CH_3CN/n\text{-}Bu_4NPF_6$ scanned at 0.1 V $s^{-1}$ (solid line) upon titration with $Hg^{2+}$ cation (dashed line). (b) Evolution of the OSWV of **6** ($c = 1 \times 10^{-4}$ M) in $CH_3CN/CH_2Cl_2$ (1/1) /$n\text{-}Bu_4NPF_6$ scanned at 0.1 V $s^{-1}$ (solid line) and scanned upon titration with $Ni^{2+}$ cation (dashed line).

the OSWV, of a new oxidation peak at more positive potential for $Ni^{2+}$ and $Hg^{2+}$ ($E_{1/2}$ = 794 mV and $\Delta E_{1/2}$ = +53 mV for $Ni^{2+}$ and $E_{1/2}$ = 766 mV and $\Delta E_{1/2}$ = +25 mV for $Hg^{2+}$) and at a more slightly shifted potential ($E_{1/2}$ = 755 mV and $\Delta E_{1/2}$ = +14 mV) for $Pb^{2+}$ (Figure 9b and Figures S72 and S73 (Supporting Information)). The same effect on the oxidation peak of the free 1,1′-bistriazolylferrocene **15** was observed upon addition of $Zn^{2+}$ ($\Delta E_{1/2}$ = +32 mV), $Hg^{2+}$ ($\Delta E_{1/2}$ = +76 mV), and $Pb^{2+}$ ($\Delta E_{1/2}$ = +22 mV) (Figures S90−S92 (Supporting Information)). In contrast, in the case of the structurally related 1,1′-bistriazolylferrocene **16**, only the addition of $Hg^{2+}$ metal cation promoted a clear evolution in the oxidation wave of the free ligand from $E_{1/2}$ = 871 mV to $E_{1/2}$ = 906 mV ($\Delta E_{1/2}$ = +35 mV) (Figure S101 (Supporting Information)).

Interestingly, addition of $Cu^{2+}$ induces the oxidation of the ferrocene moiety present in those free receptors, as was demonstrated through LSV experiments. Thus, LSV studies carried out upon addition of $Cu^{2+}$ to electrochemical solutions of such receptors showed a significant shift of the corresponding sigmoidal voltammetric wave toward cathodic currents, indicating that this metal cation promotes the oxidation of the free receptors. In contrast, the same experiments carried out upon addition of $Ni^{2+}$, $Zn^{2+}$, $Hg^{2}$, and $Pb^{2+}$ metal cations revealed a shift of the linear sweep voltammogram toward more positive potentials, which is in agreement with the complexation processes previously observed by OSWV (Figures S104, S1050, S106, and S107 (Supporting Information)).

The binding properties shown by receptor **11**, in contrast to those exhibited by the other monotriazole receptors, suggests that N3-triazole and N1-quinazolinone atoms should be involved in the complexation of the metal cation. Similarly, N3 and N3′ of the 1,1′-disubstituted bis(1,2,3-triazole) **6** should also participate in the corresponding metal cation binding processes.

*Optical Recognition.* The recognition properties of these ligands were also evaluated by UV−vis spectroscopy, taking into account that previous studies on ferrocene-based ligands have shown that their characteristic low-energy (LE) bands in the absorption spectra are perturbed upon complexation.[30]

As a general rule, addition of anions to these receptors does not promote any noticeable change in their corresponding UV−vis spectra. A similar result was also observed upon addition of metal cations to the receptors **3**, **8**, and **13**. In contrast, the behaviors shown by receptors **6** and **16**, bearing two triazole binding units, and **11**, in which a quinazolinone ring is directly attached to a triazole moiety, are completely different, although the results obtained revealed different selectivity to these specific analytes.

The UV−vis spectrum of receptor **6** in $CH_2Cl_2$ ($c = 5 \times 10^{-5}$ M) exhibits two absorption bands at $\lambda$ 325 nm ($\varepsilon$ = 2690 $M^{-1}$ $cm^{-1}$) and 430 nm ($\varepsilon$ = 570 $M^{-1}$ $cm^{-1}$), and only the addition of $Ni^{2+}$, $Hg^{2+}$, and $Pb^{2+}$ elicited significant optical responses. Thus, addition of increasing amounts of these metal cations induced the progressive appearance of a new LE band red-shifted by $\Delta\lambda$ = 11 nm in the cases of $Ni^{2+}$ and $Pb^{2+}$ (Figure 10) and $\Delta\lambda$ = 24 nm in the case of $Hg^{2+}$ (Figure S108 (Supporting Information)). In the three cases, the presence of well-defined isosbestic points are indicative of the existence of only two absorbing species in the solution. Moreover, the spectral titration data suggest a 2/1 binding model for the three metal cations with global association constants[31] of $\beta = 2.7 \times 10^7$ $M^{-2}$ for $Ni^{2+}$, $\beta = 1.9 \times 10^6$ $M^{-2}$ for $Hg^{2+}$, and $\beta = 2.9 \times 10^6$ $M^{-2}$ for $Pb^{2+}$.

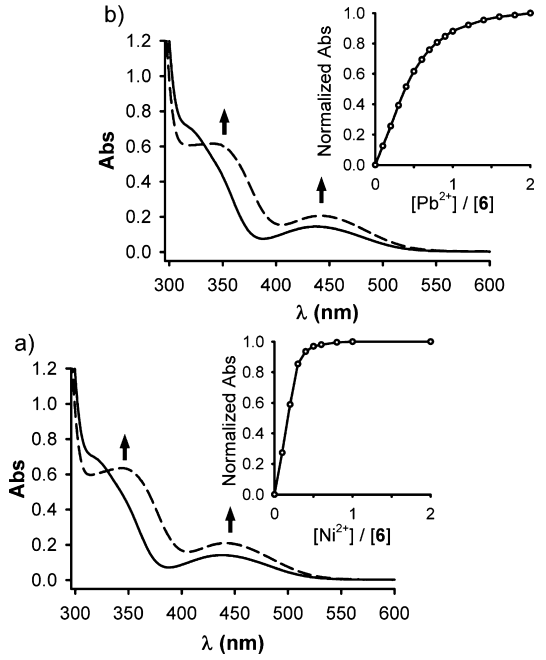


**Figure 10.** Changes in the absorption spectra of **6** (solid line) ($c = 2.5 \times 10^{-4}$ M in $CH_2Cl_2$) upon addition of increasing amounts of (a) $Ni(ClO_4)_2$ and (b) $Pb(ClO_4)_2$. The insets show the corresponding titration profiles.

On the other hand, receptor **11** in $CH_3CN$ ($c = 5 \times 10^{-5}$ M) shows two absorption bands at $\lambda$ 297 nm ($\varepsilon$ = 17220 $M^{-1}$ $cm^{-1}$) and 430 nm ($\varepsilon$ = 480 $M^{-1}$ $cm^{-1}$). However, titration experiments showed that only $Hg^{2+}$ promotes a red shift of the LE absorption band ($\Delta\lambda$ = 24 nm) (Figure S114 (Supporting


dx.doi.org/10.1021/om4002457 | Organometallics 2013, 32, 5740−5753

Information)). Well-defined isosbestic points at $\lambda$ 214 and 367 nm were found during the titration process, indicating that a clean complexation process had taken place. The resulting titration isotherm and Job plot fit nicely to a 2/1 (receptor/metal cation) binding model, the calculated global association constant[31] being $\beta = [2.86(\pm 2)] \times 10^8\ M^{-2}$.

Regarding the UV−vis spectrum of the two-armed ferrocene derivative **16**, it also exhibits two characteristic absorption bands at $\lambda$ 299 nm ($\varepsilon = 28400\ M^{-1}\ cm^{-1}$) and 437 nm ($\varepsilon = 370\ M^{-1}\ cm^{-1}$). This absorption spectrum displays noticeable changes only in the presence of $Hg^{2+}$ metal cations. Thus, addition of increasing amounts of $Hg^{2+}$ cations to a $CH_3CN$ ($c = 5 \times 10^{-5}$ M) solution of receptor **16** caused a progressive red shift of the LE band from 437 to 447 nm ($\varepsilon = 640\ M^{-1}\ cm^{-1}$) ($\Delta\lambda$ = 10 nm) (Figure S113 (Supporting Information)). A well-defined isosbestic point at 346 nm indicated the presence of a unique complex with the neutral receptor. The resulting titration profile suggests that the complexation process takes place with a 2/1 (receptor/metal cation) stoichiometry, the global association constant[31] being $\beta = 8.29 \times 10^7\ M^{-2}$.

Further evidence about the complexes formed comes from an analysis of the ESI-MS spectra, where peaks at the appropriate receptor/metal stoichiometries are observed (Figures S114−S116 (Supporting Information)). Interestingly, suitable crystals for the X-ray analysis of the complex formed between receptor **6** and $Ni^{2+}$ cation were grown, which definitely evidenced the real structure of the new complex formed. It is noteworthy that although the results obtained through the UV−vis (inset in Figure 10a) and ESI-MS (Figure 11) studies are clearly consistent with the formation of the

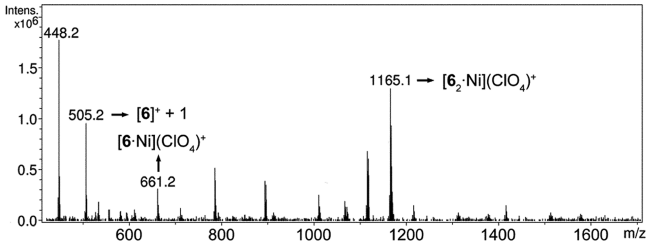


**Figure 11.** ESI-MS spectrum of an acetonitrile solution of $Ni(ClO_4)_2$ and receptor **6**, showing the formation of the $[\mathbf{6}_2{\cdot}Ni](ClO_4)_2$ species.

complex $\mathbf{6}_2{\cdot}Ni^{2+}$, the X-ray diffraction study carried out by using a crystal obtained by crystallization of the complex formed in $CHCl_3/Et_2O$ (1/5) demonstrate a real 3/1 stoichiometry (receptor/metal cation) for such a complex in the solid state (Table S29 (Supporting Information)).

Indeed we observed that the complex $[\mathbf{6}_3{\cdot}Ni](ClO_4)_2$ crystallizes as a yellow prism in the triclinic space group $P\bar{1}$. The asymmetric unit cell consists of one cation, two molecules of perchlorate, and one molecule of chloroform. In the cation, the Ni(II) ion is located in a slightly distorted octahedral coordination geometry (Figure 12 and Figure S117 and Tables S30−S34 (Supporting Information)). The Ni(II) ion is bonded by six N atoms of three bidentate ligands, each forming a five-membered chelate ring. The Ni−N bond distances in the cation range from 2.055(3) to 2.117(3) Å, and the three N−Ni—N bite angles are 78.98(10), 78.94(10), and 78.33(10)°. The two triazole rings of each ligand are almost planar, the main deviations from planes being 0.0650, 0.0819, and 0.0882 Å. The triazoles are attached between them through their C4 atoms and to the Cp rings of the ferrocenyl moieties through their N1

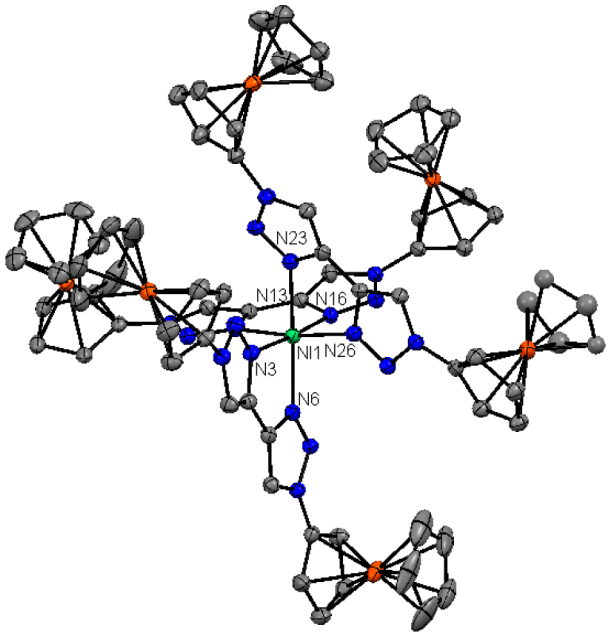


**Figure 12.** ORTEP drawings for the $[\mathbf{6}_3{\cdot}Ni^{2+}]$ complex. Thermal ellipsoids are drawn at the 35% probability level. Selected bond lengths (Å) and angles (deg): Ni(1)−N(3) = 2.055(3), Ni(1)−N(16) = 2.062(3), Ni(1)−N(26) = 2.066(3), Ni(1)−N(13) = 2.070(2), Ni(1)−N(6) = 2.080(3), Ni(1)−N(23) = 2.117(3), N(3)−Ni(1)−N(6) = 78.33(10), N(26)−Ni(1)−N(23) = 78.94(10), N(16)−Ni(1)−N(13) = 78.98(10), N(3)−Ni(1)−N(23) = 86.69(10), N(3)−Ni(1)−N(26) = 88.16(10), N(16)−Ni(1)−N(23) = 91.22(10), N(26)−Ni(1)−N(6) = 92.91(10), N(13)−Ni(1)−N(6) = 93.84(10), N(16)−Ni(1)−N(26) = 94.86(10), N(13)−Ni(1)−N(23) = 95.67(10), N(3)−Ni(1)−N(13) = 97.76(10), N(16)−Ni(1)−N(6) = 104.17(10), N(6)−Ni(1)−N(23) = 163.21(10), N(26)−Ni(1)−N(13) = 171.80(10), N(3)−Ni(1)−N(16) = 175.95(10).

atoms. The ferrocenyl moieties of two of the bidentate ligands are arranged in a *syn* conformation, while the other is in an *anti* conformation.

In the crystal structure, the cations are linked using the perchlorate anions as bridges via five intermolecular hydrogen bonds (C21−H21···O3, C21−H21···O1, C23−H23···O1, C81−H81···O2, and C83−H83···O4) forming ribbons along the *a* axis (Figure 13). The ribbons are interlinked through

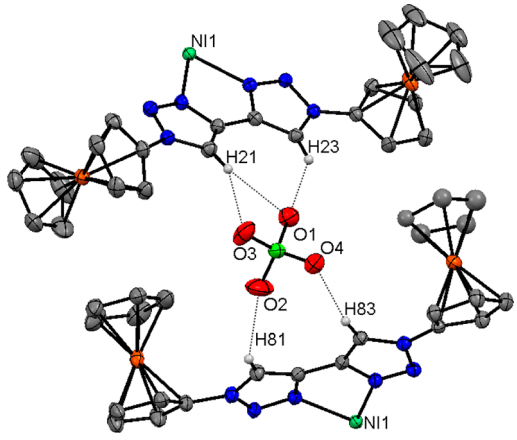


**Figure 13.** Ribbon formation in the crystal structure of the $[\mathbf{6}_3{\cdot}Ni^{2+}]$ complex. Some hydrogen atoms have been omitted for clarity.


dx.doi.org/10.1021/om4002457 | *Organometallics* 2013, 32, 5740−5753

perchlorate anions via hydrogen bonding (C51−H51···O6, C53−H53···O5, C39−H39···O8, C72−H72···O8, C77−H77···O8, and C77−H77···O6) in the *ab* and *bc* planes, producing a 3D network.

*$^1$H NMR Recognition Studies.* $^1$H NMR titration experiments were also undertaken to support the results obtained by electrochemical and spectroscopic experiments and to obtain additional information about the binding mode which takes place between the receptors and the corresponding cationic or anionic analytes.

Receptors having only one triazole unit in their structure, except for receptor **11**, do not experience any modification of their $^1$H NMR spectra upon addition of the set of metal cations tested, indicating no cation binding. In contrast, receptor **6**, in which two 1,2,3-triazole rings are directly linked, and receptor **11**, with a quinazolinone ring attached to the 4-position of the triazole ring, show noticeable $^1$H NMR responses in the presence of the appropriate cations. Thus, $^1$H NMR titration experiments carried out by using receptor **6** and $Pb^{2+}$ and $Hg^{2+}$ metal cations resulted in significant downfield shifts for the triazole protons ($\Delta\delta$ = 0.33 ppm for $Pb^{2+}$ and $\Delta\delta$ = 0.47 ppm for $Hg^{2+}$), with the ferrocenyl protons remaining essentially unaffected (Figures S118 and S120 (Supporting Information)). This downfield shift is in agreement with a decrease of electron density in the triazole rings as a consequence of the probable involvement of the N3 and N3′ triazole nitrogens in the formation of the 2/1 (receptor/metal cation) complexes.

In agreement with the electrochemical and UV−vis responses, only the titration of **11** with $Hg^{2+}$ metal cation in $CD_3CN$ resulted in considerable downfield shifts in the triazole proton ($\Delta\delta$ = 0.55 ppm) and those corresponding to the quinazolinone ring ($\Delta\delta$ around 0.25 ppm for H6, H7, and H8, and $\Delta\delta$ = 0.14 ppm for H5), while the changes in chemical shifts of ferrocenyl protons were negligible. These shifts were progressively observed upon addition of increasing amounts of $Hg^{2+}$, reaching the maximum value after addition of 0.5 equiv of the metal cation (Figure 14). This result demonstrates that two

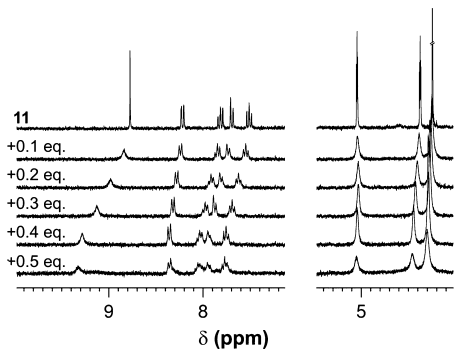


**Figure 14.** Evolution of the $^1$H NMR of **11** ($CD_3CN$, 400 MHz) after addition of 0−0.5 equiv of $Hg(OTf)_2$.

molecules of receptor **11** should be involved in the formation of the corresponding [**11**$_2$·$Hg^{2+}$] metal complex through the N3 of the triazole ring and the N1 belonging to the quinazolinone ring.

The anion binding properties toward anions was also studied by monitoring the $^1$H NMR spectral changes. For receptors **3** and **8**, bearing a single 1,2,3-triazole moiety in their structures, we performed accurate $^1$H NMR titrations in $CD_3CN$ of these compounds in the presence of increasing amounts of the appropriate anionic analyte. As shown in Figures S121−S123 and S128−S131 (Supporting Information), the most significant $^1$H NMR spectral change observed consisted of a slight downfield shift of the hydrogen atom within the triazole ring by ca. 0.05 ppm, while the protons corresponding to the ferrocene moieties were unaltered.

The same type of study carried out by using the 1,1′-disubstituted ferrocene-triazoles **15** and **16** also demonstrated that the effect promoted by the anions tested on these receptors is quite similar to that observed in the monotriazole derivatives, although the magnitude of the downfield shift corresponding to the CH triazole proton is slightly higher in these cases ($\Delta\delta$ ranges from 0.15 ppm for $HP_2O_7^{3-}$ to 0.10 ppm for $AcO^-$) (Figures S133−S140 (Supporting Information)).

The anion-sensing ability of the triazolium salts **4** and **9** was also established through $^1$H NMR titration studies. These receptors showed comparable sensitivities to the set of anions tested. Thus, the effect of the addition of up to 10 equiv of every anion in the $^1$H NMR spectrum of a solution of such receptors was very similar. Therefore, the anion recognition process did not seem to depend on the presence of any specific feature of the receptors but was due to the common cationic triazolium structure present in these derivatives. In general, it is observed that the signal corresponding to the CH-triazolium proton is shifted strongly downfield, demonstrating that these protons should be involved in the receptor−anion binding system. Moreover, the $\alpha$ protons in the monosubstituted cyclopentadienyl rings of the ferrocene moieties (N-Fc and C-Fc in **4** and N-Fc in **9**) also showed a marked downfield shift, while the $\beta$ and unsubstituted Cp protons of such ferrocenyl units showed negligible modifications with reference to those in the free receptor. As a representative example, Figure 15 shows

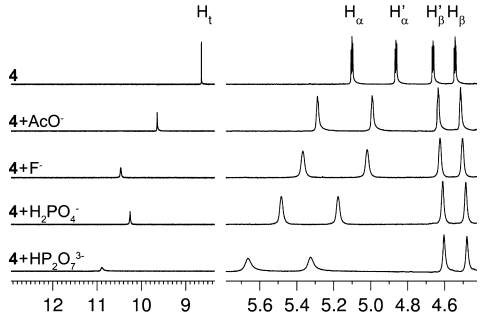


**Figure 15.** Evolution of the $^1$H NMR spectrum of **4** ($CD_3CN$, 300 MHz) upon addition of of $AcO^-$, $F^-$, $H_2PO_4^-$, and $HP_2O_7^{3-}$ anions.

the corresponding $^1$H NMR spectra obtained for **4** in the presence of the set of anions studied. Interestingly, H8 and H10 protons within the phenanthrene moiety in **9** also experienced downfield shifting upon addition of the anionic species (Figures S141−S144 (Supporting Information)), the most significant being observed in the cases of $H_2PO_4^-$ ($\Delta\delta_{H10}$ = 0.30 ppm; $\Delta\delta_{H8}$ = 0.14 ppm) (Figure S142) and $HP_2O_7^{3-}$ ($\Delta\delta_{H10}$ = 0.50 ppm; $\Delta\delta_{H8}$ = 0.23 ppm) (Figure S144).

## ■ CONCLUSIONS

Several structural motifs based on a ferrocene-triazole core have been prepared using the copper-catalyzed 1,3-dipolar cycloaddition. Starting from ferrocenyl azide, as the azido component, bisferrocene derivatives **3** and **6** linked through


dx.doi.org/10.1021/om4002457 | *Organometallics* 2013, 32, 5740−5753

one or two triazole rings have been prepared, whereas the reaction with aromatic or heteroaromatic alkynyl compounds provided the ferrocenyl derivatives **8** and **11**. Some of them have been converted into the corresponding ferrocenyltriazolium derivatives **4** and **9** by using a standard procedure. The use of 1,1′-bis(azido)ferrocene allows the formation of the trisferrocene **15**, bearing two triazole bridges, and the 1,1′-disubstituted ferrocene **16**, capped with two phenanthryltriazole fragments. The sensing properties of the prepared receptors have been studied by electrochemical and optical techniques toward anions and cations.

The most salient features derived from these studies are that receptors **3**, **6**, **15**, and **16** undergo important and, in some cases, unprecedented cathodic shifts of the oxidation peak of the ferrocene/ferrocenium redox couple in the presence of $F^-$, $AcO^-$, $H_2PO_4^-$, and $HP_2O_7^{3-}$ anions, which is due to the formation of hydrogen-bonded complexes, whereas receptor **11** undergoes deprotonation under the same electrochemical conditions. On the other hand, receptors **11** and **16** behave as dual redox and optically selective molecular sensors of $Hg^{2+}$ cations, while receptor **6** acts as an effective binding receptor for $Ni^{2+}$, $Hg^{2+}$, and $Pb^{2+}$. The isolation of the complex $[\mathbf{6}_3{\cdot}Ni^{2+}]$ as a crystalline solid allowed us to determine its X-ray structure.

## EXPERIMENTAL SECTION

**General Comments.** Commercial starting materials (ferrocene, *n*-butyllithium, ethynylferrocene, 9-ethynylphenanthrene, and 1,4-bis(trimethylsilyl)-1,3-butadiyne) were purchased from Aldrich, and they were used without further purification. Ferrocenyl azide,[6p] 1,1′-bis(azido)ferrocene,[16] 1-pyrenyl azide,[15] and 2-ethynyl-4(3*H*)-quinazolinone[14] were prepared as described previously in the literature. Melting points were determined on a Kofler hot-plate melting point apparatus and are uncorrected. $^1H$ and $^{13}C$ spectra were recorded on Bruker Avance 200, 300, 400, and 600 instruments. The following abbreviations for stating the multiplicity of the signals have been used: s (singlet), bs (broad singlet), d (doublet), t (triplet), st (pseudotriplet), m (multiplet), q (quaternary carbon). Chemical shifts refer to signals of tetramethylsilane in the case of $^1H$ and $^{13}C$ spectra. The electrospray (ESI) mass spectra were recorded on a Fisons AUTOSPEC 500 VG spectrometer. Microanalyses were performed on a Carlo Erba 1108 instrument. Cyclic voltammetry (CV) and Osteryoung square wave voltammetry (OSWV) techniques were performed with a conventional three-electrode configuration consisting of a carbon working electrode, a platinum auxiliary electrode, and a Ag/AgCl reference electrode. The experiments were carried out with a $10^{-4}$ M solution of sample in $CH_3CN$ or $CH_3CN/CH_2Cl_2$ (1/1) containing 0.1 M $(n\text{-}C_4H_9)_4NPF_6$ (TBAHP) as the supporting electrolyte. All the potential values reported are relative to the decamethylferrocene (DMFc) couple at room temperature. Deoxygenation of the solutions was achieved by bubbling nitrogen for at least 10 min, and the working electrode was cleaned after each run. The cyclic voltammograms were recorded with a scan rate of 0.1 V $s^{-1}$, while the OSWV were recorded at a scan rate of 100 mV $s^{-1}$ with a pulse hight of 10 mV and a step time of 50 ms. Typically, the receptor ($10^{-4}$ M) was dissolved in the appropriate solvent (5 mL) and TBAHP (base electrolyte) (0.194 g) was added. The guest under investigation was then added as a $2.5 \times 10^{-2}$ M solution in the appropriate solvent using a microsyringe while the electrochemical properties of the solution were monitored. DCMF was used as an external and/or internal reference both for potential calibration and for reversibility criteria. UV−vis and emission spectra were carried out in the solvents and concentrations stated in the text and in the corresponding figure captions. Quantum yield values were measured with respect to anthracene as standard ($\Phi = 0.27 \pm 0.01$) using the equation $\Phi_x/\Phi_s = (S_x/S_s)[(1 - 10^{-A_s})/(1 - 10^{-A_x})](n_s^2/n_x^2)$,[22] where x and s indicate the unknown and standard solutions, respectively, $\Phi$ is the quantum yield, $S$ is the area under the emission curve, $A$ is the absorbance at the excitation wavelength, and $n$ is the refractive index.

**General Procedure for the Preparation of 1-Ferrocenyl 4-Substituted 1*H*-1,2,3-Triazoles 3, 8, and 11.** To a mixture of ferrocenyl azide[6p] (0.25 g, 1.10 mmol), the corresponding alkynyl derivative (1.05 mmol), THF (10 mL) and water (3 mL) was added a solution of $CuSO_4{\cdot}5H_2O$ (0.03 g, 0.11 mmol) in water (4 mL). Then, a freshly prepared solution of sodium ascorbate (0.043 g, 0.22 mmol) in water (2 mL) was added dropwise and the reaction mixture was stirred at room temperature overnight. After the THF was removed under vacuum, dichloromethane (250 mL) and an aqueous solution of ammonia (15%) were added (100 mL). The mixture was stirred for 10 min to remove all the Cu(I) derivative trapped inside the product as $[Cu(NH_3)_6]^+$. The organic phase was washed with brine (100 mL) and then with water (2 × 100 mL) and filtered through a Celite pad. The solvent was removed under vacuum, and the resulting products were washed with *n*-pentane and crystallized from the appropriate solvent, yielding the corresponding triazole derivatives.

*1,4-Diferrocenyl-1H-1,2,3-triazole (**3**).*[5e] Yield: 0.428 g (89%), Mp: 236−238 °C. From $CHCl_3$/*n*-hexane at −38 °C. $\delta_H$ (200 MHz; $CDCl_3$; $Me_4Si$): 7.66 (s, 1H, H-triazole), 4.88 (st, 2H, N-Fc-$H_\alpha$), 4.77 (st, 1H, C-Fc-$H_\alpha$), 4.33 (st, 2H, C-Fc-$H_\beta$), 4.28 (st, 2H, N-Fc-$H_\beta$), 4.23 (s, 5H, N-Fc-Cp), 4.10 (s, 5H, C-Fc-Cp). $\delta_C$ (100 MHz; $CDCl_3$; $Me_4Si$): 146.8 (q), 118.0 (CH), 93.7 (q), 75.2 (q), 70.1 (CH), 69.6 (CH), 68.8 (CH), 66.7 (CH), 66.6 (CH), 61.9 (CH). ESI MS: *m*/*z* (relative intensity) 437.9 ($M^+$ + 1, 100). Anal. Calcd for $C_{22}H_{19}Fe_2N_3$: C, 60.45; H, 4.38; N, 9.61. Found: C, 60.22; H, 4.52; N, 9.36.

*1-Ferrocenyl-4-(phenanthren-9-yl)-1H-1,2,3-triazole (**8**).* Yield: 0.274 g (58%). Mp: 184−186 °C. From $CH_2Cl_2$. $\delta_H$ (600 MHz; $CDCl_3$; $Me_4Si$): 8.80 (dd, 1H, $^4J$ = 1.0 Hz, $^3J$ = 8.3 Hz), 8.73 (d, 1H, $^3J$ = 8.3 Hz), 8.46 (dd, 1H, $^4J$ = 1.2 Hz, $^3J$ = 8.3 Hz), 8.09 (s, 1H, H-triazole), 8.06 (s, 1H), 7.95 (dd, 1H, $^4J$ = 1.1 Hz, $^3J$ = 7.9 Hz), 7.72 (ddd, 1H, $^4J$ = 1.4 Hz, $^3J$ = 6.9 Hz, $^3J$ = 8.3 Hz), 7.70 (ddd, 1H, $^4J$ = 1.4 Hz, $^3J$ = 6.9 Hz, $^3J$ = 8.3 Hz), 7.66 (ddd, 1H, $^4J$ = 1.4 Hz, $^3J$ = 7.1 Hz, $^3J$ = 8.4 Hz), 7.64 (ddd, 1H, $^4J$ = 1.0 Hz, $^3J$ = 7.0 Hz, $^3J$ = 7.9 Hz), 4.96 (st, 2H, Fc-$H_\alpha$), 4.33 (st, 2H, Fc-$H_\beta$), 4.30 (s, 5H). $\delta_C$ (100 MHz; $CDCl_3$; $Me_4Si$): 146.8 (q), 131.3 (q), 130.8 (q), 130.5 (q), 130.2 (q), 128.9 (CH), 128.4 (CH), 127.2 (CH), 127.0 (CH), 126.9 (CH), 126.8 (CH), 126.5 (q), 126.2 (CH), 123.0 (CH), 122.6 (CH), 122.4 (CH), 93.8 (q), 70.3 (CH), 66.8 (CH), 62.3 (CH). ESI MS: *m*/*z* (relative intensity) 430.1 ($M^+$ + 1, 100). Anal. Calcd for $C_{26}H_{19}FeN_3$: C, 72.74; H, 4.46; N, 9.79. Found: C, 72.93; H, 4.19; N, 10.07.

*2-(1-Ferrocenyl-1H-1,2,3-triazol-4-yl)quinazolin-4(3H)-one (**11**).* Yield: 0.173 g (40%). Mp: 190−193 °C. From $CH_3CN$. $\delta_H$ (400 MHz; $CDCl_3$; $Me_4Si$): 10.18 (1H, s, NH), 8.55 (s, 1H, H-triazole), 8.35 (ddd, 1H, $^5J$ = 0.5 Hz, $^4J$ = 1.5 Hz, $^3J$ = 8.0 Hz), 7.80 (ddd, 1H, $^4J$ = 1.5 Hz, $^3J$ = 7.0 Hz, $^3J$ = 8.2 Hz), 7.74 (ddd, 1H, $^5J$ = 0.5 Hz, $^4J$ = 1.3 Hz, $^3J$ = 8.2 Hz), 7.51 (ddd, 1H, $^4J$ = 1.3 Hz, $^3J$ = 7.0 Hz, $^3J$ = 8.0 Hz), 4.94 (st, 2H, Fc-$H_\alpha$), 4.36 (st, 2H, Fc-$H_\beta$), 4.26 (s, 5H, Fc-Cp). $\delta_C$ (75 MHz; $CDCl_3$; $Me_4Si$): 161.0 (q), 148.9 (q), 144.5 (q), 141.6 (q), 134.8 (CH), 127.3 (CH), 127.1 (CH), 126.9 (CH), 123.4 (CH), 122.1 (q), 92.9 (q), 70.4 (q), 67.3 (CH), 62.2 (CH). ESI MS: *m*/*z* (relative intensity) 420.1 ($M^+$ + Na, 100). Anal. Calcd for $C_{20}H_{15}FeN_5O$: C, 60.48; H, 3.81; N, 17.63. Found: C, 60.22; H, 3.55; N, 17.92.

**Synthesis of 1,1′-Diferrocenyl-1*H*,1′*H*-4,4′-bi(1,2,3-triazole) (6).** To a mixture of ferrocenyl azide (0.3 g, 1.32 mmol), 1,4-bis(trimethylsilyl)butadiyne (0.117 g, 0.60 mmol), THF (20 mL), and water (5 mL) was added a solution of $CuSO_4{\cdot}5H_2O$ in water (5 mL). Then, a solution of tetrabutylammonium fluoride hydrate (0.345 g, 1.32 mmol) and sodium L-ascorbate (0.048 g, 0.24 mmol) in water (10 mL) was slowly added via syringe, ensuring that the needle tip was introduced into the solution. The reaction mixture was stirred at room temperature for 3 days. Afterward, the THF was removed under vacuum, and chloroform (250 mL) and a 15% aqueous solution of ammonia (100 mL) were added. The mixture was stirred for 10 min to remove all the Cu(II) derivate trapped inside the product as $[Cu(NH_3)_6]^{2+}$. The organic phase was washed with brine (100 mL) and then with water (2 × 100 mL) and filtered through a Celite pad. The solvent was removed under vacuum, and the resulting residue was


dx.doi.org/10.1021/om4002457 | *Organometallics* 2013, 32, 5740−5753

triturated with ethanol, collected by filtration, and crystallized from $CHCl_3$/*n*-hexane at −38 °C, yielding 0.079 g (26%) of **6**. Mp: 240−242 °C. $\delta_H$ (400 MHz; $CDCl_3$; $Me_4Si$), 8.35 (s, 1H, H-triazole), 4.93 (st, 2H, Fc-$H_\alpha$), 4.32 (st, 2H, Fc-$H_\beta$), 4.25 (s, 5H, Fc). $\delta_C$ (100 MHz; $CDCl_3$): 119.9 (CH), 70.2 (q), 66.8 (CH), 62.0 (CH). FAB$^+$ MS: *m*/*z* (relative intensity) 505.3 ($M^+$ + 1, 100). Anal. Calcd for $C_{24}H_{20}Fe_2N_6$: C, 57.18; H, 4.00; N, 16.67. Found: C, 56.87; H, 4.24; N, 16.38.

**General Procedure for the Preparation of 3-Methyl-1*H*-1,2,3-triazolium Tetrafluoroborates 4 and 9.** A solution of the appropriate triazole derivative (0.57 mmol) and trimethyloxonium tetrafluoroborate ($Me_3OBF_4$) (0.126 g, 0.85 mmol) were stirred under a nitrogen atmosphere in dry $CH_2Cl_2$ (50 mL). After the solvent was removed under reduced pressure, acetone (2 mL) and diethyl ether (10 mL) were added and the mixture was stirred for 1 h. The resulting solid was then crystallized from the appropriate solvent to give the corresponding triazolium tetrafluoroborate.

*Synthesis of 1,4-Diferrocenyl-3-methyl-1H-1,2,3-triazolium Tetrafluoroborate (**4**).* Yield: 46%. Mp: 203−206 °C. $\delta_H$ (300 MHz; $CD_3CN$; $Me_4Si$): 8.63 (s, 1H, H-triazole), 5.08 (st, 2H, N-Fc-$H_\alpha$), 4.85 (st, 1H, C-Fc-$H_\alpha$), 4.65 (st, 2H, C-Fc-$H_\beta$), 4.53 (st, 2H, N-Fc-$H_\beta$), 4.34 (s, 5H, N-Fc-Cp), 4.31 (s, 5H, C-Fc-Cp), 4.24 (s, 3H, N-$CH_3$). $\delta_H$ (200 MHz; $CDCl_3$; $Me_4Si$) 9.13 (s, 1H, H-triazole), 5.26 (st, 2H, N-Fc-$H_\alpha$), 4.97 (st, 2H, C-Fc-$H_\alpha$), 4.60 (st, 2H, C-Fc-$H_\beta$), 4.48 (st, 2H, N-Fc-$H_\beta$), 4.36 (s, 5H, N-Fc-Cp), 4.30 (s, 8H, C-Fc-Cp + N-$CH_3$). $\delta_H$ (400 MHz; acetone-$d_6$; $Me_4Si$): 9.29 (s, 1H), 5.3 (st, 2H), 5.08 (st, 2H), 4.68 (st, 2H), 4.57 (st, 2H), 4.51 (s, 3H), 4.38 (s, 5H), 4.37 (s, 5H). $\delta_C$ (50 MHz; acetone-$d_6$; $Me_4Si$): 145.6 (q), 126.5 (CH), 92.7 (q), 72.2 (CH), 71.9 (CH), 71.1 (CH), 69.9 (CH), 69.4 (CH), 66.8 (q), 63.6 (CH), 40.0 ($CH_3$). ESI MS: *m*/*z* (relative intensity) 452.1 ($M^+ - BF_4$, 100). Anal. Calcd for $C_{23}H_{22}BF_4Fe_2N_3$: C, 51.26; H, 4.11; N, 7.80. Found: C, 51.54; H, 4.34; N, 8.09.

*Synthesis of 1-Ferrocenyl-4-(phenanthren-9-yl)-3-methyl-1H-1,2,3-triazolium Tetrafluoroborate (**9**).* Yield: 53%. Mp: 167−169 °C. $\delta_H$ (600 MHz; $CDCl_3$; $Me_4Si$): $\delta$ 8.80 (d, 1H, $^3J$ = 8.3), 8.71 (d, 1H, $^3J$ = 8.4), 8.69 (s, 1H), 8.42 (s, 1H), 8.11 (1H, d, $^3J$ = 7.1), 7.81−7.79 (m, 1H), 7.75−7.73 (m, 1H), 7.68−7.65 (2H, m), 7.41 (1H, d, J=7.2), 5.23 (bs, 2H), 4.49 (bs, 7H), 4.08 (s, 3H). $\delta_H$ (300 MHz; acetone-$d_6$; $Me_4Si$): 9.57 (s, 1H), 9.06 (d, 1H, $^3J$ = 8.2 Hz), 9.01 (d, 1H, $^3J$ = 8.4 Hz), 8.35 (s, 1H,), 8.14 (d, 1H, $^3J$ = 7.8 Hz), 7.96−7.86 (m, 3H), 7.81 (ddd, 1H, $^4J$ = 0.9 Hz, $^3J$ = 7.1 Hz, $^3J$ = 7.9 Hz), 7.74 (ddd, 1H, $^4J$ = 1.0 Hz, $^3J$ = 7.1 Hz, $^3J$ = 8.1 Hz), 5.39 (st, 2H, Fc-$H_\alpha$), 4.67 (st, 2H, Fc-$H_\beta$), 4.49 (s, 5H, Fc-Cp), 4.35 (s, 3H, N-$CH_3$). $\delta_C$ (75 MHz, $CDCl_3$; $Me_4Si$): $\delta$ 142.5 (q), 134.2 (CH), 131.4 (q), 130.7 (q), 130.6 (CH), 130.3 (q), 129.4 (CH), 129.2 (q), 128.7 (q), 128.1 (CH), 127.8 (2C, CH), 124.0 (CH), 123.8 (CH), 122.5 (CH), 116.5 (CH), 92.7 (q), 72.5 (Fc-Cp), 69.7 (Fc-CH$\beta$), 64.7 (Fc-CH$\alpha$), 38.7 (N−$CH_3$). $\delta_C$ (75 MHz; acetone-$d_6$; $Me_4Si$): 142.7 (q), 133.4, 132.1 (q), 131.2 (q), 130.9 (q), 130.3 (CH), 130.2 (CH), 130.0 (CH), 129.7 (q), 128.7 (CH), 128.6 (CH), 128.5 (CH), 125.9 (CH), 124.3 (CH), 123.7 (CH), 118.9 (q), 92.87 (q), 71.8 (CH), 69.4 (CH), 63.9 (CH), 39.0 ($CH_3$). ESI MS: *m*/*z* (relative intensity) 444.3 ($M^+ - BF_4$, 100). Anal. Calcd for $C_{27}H_{22}BF_4FeN_3$: C, 61.06; H, 4.17; N, 7.91. Found: C, 60.79; H, 4.47; N, 7.70.

**Synthesis of 4-Ferrocenyl-1-(pyren-1-yl)-1*H*-1,2,3-triazole (13).** To a mixture of 1-pyrenyl azide[15] (**12**; 0.250 g, 1.03 mmol), and ethynylferrocene (**2**; 0.227 g, 1.08 mmol) in THF (10 mL) and water (3 mL) was added a solution of $CuSO_4{\cdot}5H_2O$ (0.03 g, 0.11 mmol) in water (4 mL). Then, a freshly prepared solution of sodium ascorbate (0.043 g, 0.22 mmol) in water (2 mL) was added dropwise and the reaction mixture was stirred at room temperature overnight. After the THF was removed under vacuum, dichloromethane (250 mL) and an aqueous solution of ammonia (15%) were added (100 mL). The mixture was stirred for 10 min to remove all the Cu(I) derivative trapped inside the product as $[Cu(NH_3)_6]^+$. The organic phase was washed with brine (100 mL) and then with water (2 × 100 mL) and filtered through a Celite pad. The solvent was removed under vacuum, and the resulting products were washed with *n*-pentane and crystallized from $CHCl_3$/*n*-hexane, giving the 1,4-disubstituted triazole **13** in 59% yield (0.275 g). Mp: 226−228 °C. $\delta_H$ (400 MHz; $CDCl_3$; $Me_4Si$): 8.32−8.29 (m, 2H), 8.27 (d, 1H, $^3J$ = 7.6 Hz), 8.22 (d, 1H, $^3J$ = 9.0 Hz), 8.19−8.15 (m, 2H), 8.13 (d, 1H, $^3J$ = 8.1 Hz), 8.10 (t, 1H, $^3J$ = 7.6 Hz), 7.99 (s, 1H), 7.93 (d, 1H, $^3J$ = 9.2 Hz), 4.88 (st, 2H, Fc-$H_\alpha$), 4.39 (st, 2H, Fc-$H_\beta$), 4.20 (s, 5H, Fc-Cp). $\delta_C$ (100 MHz; $CDCl_3$; $Me_4Si$): 147.9 (q), 133.1 (q), 132.0 (q), 131.6 (q), 130.6 (CH), 129.8 (CH), 127.9 (CH), 127.7 (q), 127.3 (CH), 127.2 (q), 127.0 (CH), 126.0 (q), 125.6 (CH), 125.1 (q), 124.3 (CH), 122.9 (CH), 122.1 (CH), 78.1 (q), 70.7 (CH), 69.9 (CH), 67.8 (CH). ESI MS: *m*/*z* (relative intensity) 454.3 ($M^+$ + 1, 100). Anal. Calcd for $C_{28}H_{19}FeN_3$: C, 74.19; H, 4.22; N, 9.27. Found: C, 74.46; H, 4.51; N, 8.99.

**General Procedure for the Preparation of 1,1′-Disubstituted Ferrocene-Triazoles 15 and 16.** To a mixture of 1,1′-diazidoferrocene[16] (0.25 g, 0.9 mmol), the corresponding alkynyl derivative (1.8 mmol), THF (10 mL), and water (2 mL) was added a solution of $CuSO_4{\cdot}5H_2O$ (0.05 g, 0.19 mmol) in water (3 mL). Then, a freshly prepared solution of sodium ascorbate (0.07 g, 0.37 mmol) in water (5 mL) was added dropwise and the reaction mixture was stirred at room temperature for 72 h. The resulting products were washed with *n*-pentane and crystallized from $CHCl_3$/*n*-hexane at −38 °C, yielding the corresponding bis(triazolyl)ferrocene derivatives.

*1,1′-Bis[(4-ferrocenyl)-1H-1,2,3-triazol-1-yl]ferrocene (**15**).*[5e] Yield: 0.388 g (61%). Mp: 206−209 °C. $\delta_H$ (400 MHz; $CDCl_3$; $Me_4Si$): 7.63 (s, 2H), 4.87 (st, 4H, N-Fc-$H_\alpha$), 4.72 (st, 4H, C-Fc-$H_\alpha$), 4.38 (st, 4H, N-Fc-$H_\beta$), 4.29 (st, 4H, C-Fc-$H_\beta$), 4.07 (s, 10H, Cp). $\delta_C$ (100 MHz; $CDCl_3$; $Me_4Si$): 147.2 (q), 118.4 (CH), 95.2 (q), 74.7 (q), 69.5 (CH), 68.8 (CH), 68.4 (CH), 66.8 (CH), 64.0 (CH). ESI MS: *m*/*z* (relative intensity) 688.2 ($M^+$ + 1, 100). Anal. Calcd for $C_{34}H_{28}Fe_3N_6$: C, 59.34; H, 4.10; N, 12.21. Found: C, 59.56; H, 3.81; N, 12.48.

*1,1′-Bis{[4-(phenanthren-9-yl)]-1H-1,3,4-triazol-1-yl}ferrocene (**16**).* Yield: 0.238 g (38%). Mp: 234−236 °C. $\delta_H$ (600 MHz; $CDCl_3$; $Me_4Si$): 8.63 (d, 1H, $^3J$ = 8.2 Hz), 8.57 (d, 2H, $^3J$ = 8.3 Hz), 8.41 (d, 2H, $^3J$ = 8.2 Hz), 8.03 (s, 2H, H-triazole), 7.91 (s, 2H), 7.62 (d, 2H, $^3J$ = 7.9 Hz), 7.59 (ddd, 2H, $^4J$ = 1.2 Hz, $^3J$ = 7.1 Hz, $^3J$ = 8.3 Hz), 7.57 (ddd, 2H, $^4J$ = 1.2 Hz, $^3J$ = 7.0 Hz, $^3J$ = 8.2 Hz), 7.51 (ddd, 2H, $^4J$ = 1.2 Hz, $^3J$ = 7.0 Hz, $^3J$ = 8.2 Hz), 7.44 (m, 2H), 5.10 (4H, st), 4.50 (4H, st). $\delta_C$ (100 MHz; $CDCl_3$; $Me_4Si$): 147.2 (q), 131.2 (q), 130.7 (q), 130.4 (q), 129.9 (q), 128.9 (CH), 128.5 (CH), 127.0 (CH), 126.8 (CH), 126.6 (CH), 126.5 (CH), 126.1 (CH), 126.0 (q), 122.9 (CH), 122.4 (CH), 122.2 (CH), 95.4 (q), 68.6 (CH), 64.2 (CH). ESI MS: *m*/*z* (relative intensity) 673.3 ($M^+$ + 1, 100). Anal. Calcd for $C_{42}H_{28}FeN_6$: C, 75.00; H, 4.20; N, 12.50. Found: C, 75.27; H, 3.89; N, 12.63.

**Preparation of the Complex $[6_3{\cdot}Ni](ClO_4)_2$.** The complex was obtained by slow diffusion of diethyl ether into a mixture of **6** (0.050 mg, 0.1 $\mu$mol) in $CH_3Cl$ (1 mL) and $NiClO_4{\cdot}6H_2O$ (0.018 mg, 0.05 $\mu$mol) in $CH_3CN$ (1 $\mu$L). The yellow crystals obtained were suitable for X-ray diffraction analysis. Mp: 203−206 °C dec. Anal. Calcd for $C_{72}H_{60}Cl_2Fe_6N_{18}NiO_8$: C, 48.86; H, 3.42; N, 14.24. Found: C, 48.49; H, 3.16; N, 14.56.

**X-ray Structural Analysis.** Suitable single crystals for X-ray diffraction were mounted in inert oil on a glass fiber and transferred to a Bruker Smart APEX diffractometer equipped with a CCD detector. Measurements were carried out at 100(2) K using graphite-monochromated Mo K$\alpha$ radiation ($\lambda$ = 0.71073 Å) in $\omega$-scan mode. The SMART program package was used to determine unit-cell parameters and to collect data. The raw frame data were processed using SAINT and SADABS to yield the reflection data files. Subsequent calculations were carried out using the SHELXTL program suite. Structures were solved by direct methods (Patterson methods in the case of compound **9**), and all non-hydrogen atoms were refined anisotropically on $F^2$ by full-matrix least-squares techniques. All hydrogen atoms were initially located in a difference Fourier map and refined using a standard riding model unless otherwise stated. Diffraction data for compounds **4**, **8**, **9**, **11**, **13**, and $[6_3{\cdot}Ni^{2+}]$ are given in Tables S2, S3, and S29 (Supporting Information).

*Special Features and Exceptions.* Compound **4**: the hydrogen atoms of the methyl group were refined using a rigid model. Compound **9**: the structure was solved by Patterson methods. The hydrogen atoms of the methyl group were refined using a rigid model.


dx.doi.org/10.1021/om4002457 | *Organometallics* 2013, 32, 5740−5753

One tetrafluoroborate anion was disordered over two positions (66/33), and all the atoms of both components were refined anisotropically. Compound **11**: the N4−H04 hydrogen atom was refined freely. Complex $[\mathbf{6}_3\cdot Ni](ClO_4)_2$: the cyclopentadienyl C76-ring of one ferrocenyl moeity was disordered over two positions of approximately equal occupancy. The disordered carbon atoms of both components were refined isotropically and their hydrogens calculated. One perchlorate anion was also disordered over two equally occupied positions. The disordered chlorine atoms of both components were refined anisotropically and the oxygen atoms isotropically. The chlorine atoms of a solvent molecule of chloroform were disordered over two positions (84/16), and those of the major component were refined anisotropically. The largest residual electron density peak (2.00 e $Å^{-3}$) present 0.90 Å from O7 may be due to residual absorption or unidentified disorder effects.

## ■ ASSOCIATED CONTENT

### Ⓢ Supporting Information

Figures, tables, and CIF files giving one- and two-dimensional NMR spectra, electrochemical, UV−vis, emission, and $^1H$ NMR titration data, ESI-MS spectra, and X-ray diffraction data. This material is available free of charge via the Internet at http://pubs.acs.org.

## ■ AUTHOR INFORMATION

### Corresponding Author

*E-mail: pmolina@um.es (P.M.); atarraga@um.es (A.T.).

### Notes

The authors declare no competing financial interest.

## ■ ACKNOWLEDGMENTS

We gratefully acknowledge financial support from the MICINN-Spain, FEDER Project CTQ 2011-27175, and Fundación Séneca (Agencia de Ciencia y Tecnología de la Región de Murcia) Project 04509/GERM/06 (Programa de Ayudas a Grupos de Excelencia de la Región de Murcia, Plan Regional de Ciencia y Tecnología 2007/2010).

## ■ REFERENCES

(1) Huisgen, R.; Szeimies, G.; Moebius, L. *Chem. Ber.* **1967**, *100*, 2494−2507.

(2) (a) Rostovtsev, V.; Green, L. G.; Fokin, V. V.; Sharpless, K. B. *Angew. Chem., Int. Ed.* **2002**, *41*, 2596−2599. (b) Tornoe, C. V.; Christensen, C.; Medal, M. *J. Org. Chem.* **2002**, *67*, 3057−3064.

(3) Kolb, H. C.; Finn, M. G.; Sharpless, K. B. *Angew. Chem., Int. Ed.* **2001**, *40*, 2004−2021.

(4) (a) Moses, J. E.; Moorhouse, A. D. *Chem. Soc. Rev.* **2007**, *36*, 1249−1262. (b) Nandivada, H.; Jiang, X.; Lahann, J. *Adv. Mater.* **2007**, *19*, 2197−2028. (c) Ou, T.-M.; Lu, Y.-J.; Tan, J.-H.; Huang, Z.-S.; Wong, K.-Y.; Gu, L.-Q. *Chem. Med. Chem.* **2008**, *3*, 690−713.

(5) (a) Casas-Solvas, J. M.; Vargas-Berenguer, A.; Capitan-Vallvey, L. F.; Santoyo-Gonzalez, F. *Org. Lett.* **2004**, *6*, 3687−3690. (b) Gasser, G.; Hüsken, N.; Köster, S. D.; Metzler-Nolte, N. *Chem. Commun.* **2008**, 3675−3677. (c) Köster, S. D.; Dittrich, J.; Gasser, G.; Hüsken, N.; Henao-Castañeda, I. C.; Jios, J. L.; Della Vedova, C. O.; Metzler-Nolte, N. *Organometallics* **2008**, *27*, 6326−6332. (d) Badeche, S.; Daran, J.-C.; Ruiz, J.; Astruct, D. *Inorg. Chem.* **2008**, *47*, 4903−4908. (e) Siemeling, U.; Rother, D. *J. Organomet. Chem.* **2009**, *694*, 1055−1058.

(6) (a) Bronisz, R. *Inorg. Chem.* **2005**, *44*, 4463−4465. (b) Li, Y.; Huffman, J. C.; Flood, A. H. *Chem. Commun.* **2007**, *26*, 2692−2694. (c) Chan, T. R.; Hilgraf, R.; Sharpless, K. B.; Fokin, V. V. *Org. Lett.* **2004**, *6*, 2853−2855. (d) Chang, K.-C.; Su, I.-H.; Senthilvelan, A.; Chung, W.-S. *Org. Lett.* **2007**, *9*, 3363−3366. (e) David, O.; Maisonneuve, S.; Xie, J. *Tetrahedron Lett.* **2007**, *48*, 6527−6530. (f) Chang, K.-C.; Su, I.-H.; Lee, G.-H.; Chung, W.-S. *Tetrahedron Lett.* **2007**, *48*, 7274−7278. (g) Ornelas, C.; Aranzaes, J. R.; Salmon, L.; Astruc, D. *Chem. Eur. J.* **2008**, *14*, 50−64. (h) Ornelas, C.; Salmon, L.; Aranzaes, J. R.; Astruc, D. *Chem. Commun.* **2007**, 4946−4948. (i) Huang, S.; Clark, R. J.; Zhu, L. *Org. Lett.* **2007**, *9*, 4999−5002. (j) David, O.; Maisonneuve, S.; Xie. *Tetrahedron Lett.* **2007**, *48*, 6527−6530. (k) Park, S. Y.; Yoon, J. H.; Hong, C. S.; Souane, R.; Kim, J. S.; Mattews, S. E.; Vicens, J. *J. Org. Chem.* **2008**, *73*, 8212−8218. (l) Hung, H.-C.; Cheng, C.-W.; Ho, I.-T.; Cheng, W.-S. *Tetrahedron Lett.* **2009**, *50*, 302−305. (m) Suijkerbuijk, B. M. J. M.; Aerts, B. N.; Dijkstra, H. P.; Lutz, M.; Spek, A. L.; van Koten, G.; Klein Gebbink, R. J. M. *Dalton Trans.* **2007**, 1273−1276. (n) Crowley, J. D.; Bandeen, P. H.; Hanton, L. R. *Polyhedron* **2010**, *29*, 70−83. (o) Kilpin, K. J.; Crowley, J. D. *Polyhedron* **2010**, *29*, 3111−3117. (p) Romero, T.; Orenes, R. A.; Espinosa, A.; Tárraga, A.; Molina, P. *Inorg. Chem.* **2011**, *50*, 8214−8224. (q) Otón, F.; González, M. C.; Espinosa, A.; Tárraga, A.; Molina, P. *Organometallics* **2012**, *31*, 2085−2096.

(7) (a) Kumar, A.; Pandey, P. S. *Org. Lett.* **2008**, *10*, 165−168. (b) Haridas, V.; Lal, K.; Sharma, Y. K.; Upreti, S. *Org. Lett.* **2008**, *10*, 1645−1647. (c) Horne, W. S.; Yadav, M. K.; Scout, C. D.; Ghadiri, M. R. *J. Am. Chem. Soc.* **2004**, *126*, 15366−15367. (d) Li, Y.; Flood, A. H. *Angew. Chem., Int. Ed.* **2008**, *47*, 2649−2652. (e) Juwarker, H.; Lenhardt, J. M.; Pham, D. M.; Craig, S. L. *Angew. Chem., Int. Ed.* **2008**, *47*, 3740−3743. (f) Meudtner, R. M.; Hecht, S. *Angew. Chem., Int. Ed.* **2008**, *47*, 4926−4930. (g) Ornelas, C.; Aranzaes, J. R.; Cloutet, E.; Alves, S.; Astruc, D. *Angew. Chem., Int. Ed.* **2007**, *46*, 872−877. (h) Hua, Y.; Flood, A. H. *Chem. Soc. Rev.* **2010**, *39*, 1262−1271. (i) Romero, T.; Caballero, A.; Tárraga, A.; Molina, P. *Org. Lett.* **2009**, *11*, 3466−3469. (j) Otón, F.; González, M. C.; Espinosa, A.; Ramirez de Arellano, C.; Tárraga, A.; Molina, P. *J. Org. Chem.* **2012**, *77*, 10083−10092. (k) Yu, G.; Zhang, Z.; Han, C.; Xue, M.; Zhou, Q.; Huang, F. *Chem. Commun.* **2012**, *48*, 2958−2960.

(8) Ornelas, C.; Aranzaes, J. R.; Cloutet, E.; Alves, S.; Astruc, D. *Angew. Chem., Int.* **2007**, *46*, 872−877.

(9) Li, Y.; Flood, A. H. *J. Am. Chem. Soc.* **2008**, *130*, 12111−12122.

(10) (a) Kolb, H. C.; Sharpless, K. B. *Drug Discovery Today* **2003**, *8*, 1128−1137. (b) Bourne, Y.; Kolb, H. C.; Radic, Z.; Sharpless, K. B.; Taylor, P.; Marchot, P. *Proc. Natl. Acad. Sci. U.S.A.* **2004**, *101*, 1449−1454. (c) Brik, A.; Alexandratos, J.; Lin, Y. C.; Elder, J. H.; Olson, A. J.; Wlodawer, A.; Goodsell, D. S.; Wong, C. H. *Chem. Biochem.* **2005**, *6*, 1167−1169. (d) Bock, V. D.; Speijer, D.; Hiemstra, H.; van Maarseveen, J. H. *Org. Biomol. Chem.* **2007**, *5*, 971−975. (e) Pokorski, J. K.; Jenkins, L. M. M.; Feng, H. Q.; Durell, S. R.; Bai, Y. W.; Appella, D. H. *Org. Lett.* **2007**, *9*, 2381−2383.

(11) For reviews see: (a) Molina, P.; Tárraga, A.; Caballero, A. *Eur. J. Inorg. Chem.* **2008**, 3401−3417. (b) Molina, P.; Tárraga, A.; Alfonso, M. *Eur. J. Org. Chem.* **2011**, 4505−4518.

(12) (a) López, J. L.; Tárraga, A.; Espinosa, A.; Velasco, M. D.; Molina, P.; Lloveras, V.; Vidal-Gancedo, J.; Rovira, C.; Veciana, J.; Evans, D. J.; Wurst, K. *Chem. Eur. J.* **2004**, *10*, 1815−1826. (b) Caballero, A.; Martínez, R.; Lloveras, V.; Ratera, I.; Vidal-Gancedo, J.; Wurst, K.; Tárraga, A.; Molina, P.; Veciana, J. *J. Am. Chem. Soc.* **2005**, *127*, 15666−15667. (c) Martínez, R.; Espinosa, A.; Tárraga, A.; Molina, P. *Org. Lett.* **2005**, *7*, 5869−5872. (d) Caballero, A.; Lloveras, V.; Curiel, D.; Tárraga, A.; Espinosa, A.; García, R.; Vidal-Gancedo, J.; Rovira, C.; Wurst, K.; Molina, P.; Veciana, J. *Inorg. Chem.* **2007**, *46*, 825−838. (e) Zapata, F.; Caballero, A.; Espinosa, A.; Tárraga, A.; Molina, P. *Org. Lett.* **2007**, *9*, 2385−2388. (f) Zapata, F.; Caballero, A.; Espinosa, A.; Tárraga, A.; Molina, P. *Org. Lett.* **2008**, *10*, 41−44. (g) Zapata, F.; Caballero, A.; Espinosa, A.; Tárraga, A.; Molina, P. *Org. Lett.* **2007**, *9*, 2385−2388. (h) Martínez, R.; Espinosa, A.; Tárraga, A.; Molina, P. *Tetrahedron* **2008**, *64*, 2184−2191.

(13) Ganesh, V.; Sudhir, V. S.; Kundu, T.; Chandrasekaran, S. *Chem. Asian J.* **2011**, *6*, 2670−2694.

(14) Bergman, J.; Romero, I. *Arkivoc* **2009**, *vi*, 191−195.

(15) Ouchi, A.; Awe, B. Z. S.; Hatsuda, R.; Ogura, R.; Ishii, T.; Araki, Y.; Ito, O. *J. Phys. Chem. A* **2004**, *108*, 9584−9592.

(16) (a) Tárraga, A.; Otón, F.; Espinosa, A.; Velasco, M. D.; Molina, P.; Evans, D. J. *Chem. Commun.* **2004**, 458−459. (b) Otón, F.; Tárraga, A.; Molina, P. *Org. Lett.* **2006**, *8*, 2107−2110. (c) Otón, F.; Espinosa,

A.; Tárraga, A.; Ramírez de Arellano, C.; Molina, P. *Chem. Eur. J.* **2007**, *13*, 5742−5752.
(17) (a) Gelin, F.; Thummel, R. P. *J. Org. Chem.* **1992**, *57*, 3780−3783. (b) Inouye, M.; Hyodo, Y.; Nakazumi, H. *J. Org. Chem.* **1999**, *64*, 2704−2710. (c) Romero, T.; Caballero, A.; Espinosa, A.; Tárraga, A.; Molina, P. *Dalton Trans.* **2009**, 2121−2129.
(18) The criteria applied for reversibility was a separation of ∼60 mV between cathodic and anodic peaks, a ratio of 1.0 ± 0.1 for the intensities of the cathodic and anodic currents $I_c/I_a$, and no shift of the half-wave potentials with varying scan rates.
(19) Farrel, T.; Meyer-Friedrichsen, T.; Malessa, M.; Haase, D.; Saak, W.; Asselberghs, I.; Wostyn, K.; Clays, K.; Persoons, A.; Heck, J.; Manning, A. R. *J. Chem. Soc., Dalton Trans.* **2001**, 29−36 and references cited therein.
(20) (a) Sohn, Y. S.; Hendrickson, D. N.; Gray, M. B. *J. Am. Chem. Soc.* **1971**, *93*, 3603−3619. (b) Sanderson, C. T.; Quinian, J. A.; Conover, R. C.; Johnson, M. K.; Murphy, M.; Dluhy, R. A.; Kuntal, C. *Inorg. Chem.* **2005**, *44*, 3283−3289. (c) Gao, L.-B.; Zhang, L.-Y.; Shi, L.-X.; Cheng, Z.-N. *Organometallics* **2005**, *24*, 1678−1684.
(21) (a) Barlow, S.; Bunting, H. E.; Ringham, C.; Green, J. C.; Bublitz, G. U.; Boxer, S. G.; Perry, J. W.; Marder, S. R. *J. Am. Chem. Soc.* **1999**, *121*, 3715−3723. (b) Yamaguchi, Y.; Ding, W.; Sanderson, C. T.; Borden, M. L.; Morgan, M. J.; Kutal, C. *Coord. Chem. Rev.* **2007**, *251*, 515−524.
(22) (a) de Silva, A. P.; Gunaratne, H. Q. N.; Gunnlaugsson, T.; Huxley, A. J.; MacCoy, C. P.; Rademacher, J. T.; Rice, T. E. *Chem. Rev.* **1997**, *97*, 1515−1566. (b) Valeur, B. *Molecular Fluorescence Principles and Applications*; Wiley-VCH: Weinheim, Germany, 2002. (c) *Fluorescent Chemosensors for Ion and Molecular Recognition*; Czarnik, A. W., Ed.; American Chemical Society: Washington, DC, 1993.
(23) The fluorescence quantum yields were measured with respect to anthracene as standard (Φ = 0.27): Dawson, W. R.; Windsor, M. W. *J. Phys. Chem.* **1968**, *72*, 3251−3260.
(24) For $AcO^-$ see: (a) Sola, A.; Tárraga, A.; Molina, P. *Dalton Trans.* **2012**, *41*, 8401−8509. (b) Sola, A.; Orenes, R. A.; García, M. A.; Claramunt, R. M.; Alkorta, I.; Elguero, J.; Tárraga, A.; Molina, P. *Inorg. Chem.* **2011**, *50*, 4212−4220. For $H_2PO_4^-$, and $HP_2O_7^{3-}$ see: (c) Zapata, F.; Caballero, A.; Tárraga, A.; Molina, P. *J. Org. Chem.* **2010**, *75*, 162−169. (d) Curiel, D.; Espinosa, A.; Más-Montoya, M.; Sánchez, G.; Tárraga, A.; Molina, P. *Chem. Commun.* **2009**, 7539−7541. For $HSO_4^-$ see: (e) Alfonso, M.; Espinosa, A.; Tárraga, A.; Molina, P. *Chem. Commun.* **2012**, *48*, 6848−6850. (f) Romero, T.; Espinosa, A.; Tárraga, A.; Molina, P. *Supramol. Chem.* **2012**, *24*, 826−832. (g) Alfonso, M.; Tárraga, A.; Molina, P. *Org. Lett.* **2011**, *13*, 6432−6435.
(25) $Li^+$, $K^+$, $Mg^{2+}$, $Ni^{2+}$, $Cd^{2+}$, and $Pb^{2+}$ were added as perchlorate salts, while $Na^+$, $Ca^{2+}$, $Cu^{2+}$, $Zn^{2+}$, and $Hg^{2+}$ were added as triflate salts.
(26) The OSWV technique has been employed to obtain well-resolved potential information, while the individual redox processes are poorly resolved in the CV experiments in which individual $E_{1/2}$ potentials cannot be easily or accurately extracted from these data: (a) Serr, B. R.; Andersen, K. A.; Elliot, C. M.; Anderson, O. P. *Inorg. Chem.* **1988**, *27*, 4499−4504. (b) Richardson, D. E.; Taube, H. *Inorg. Chem.* **1981**, *20*, 1278−1285.
(27) (a) Kaifer, A. E.; Mendoza, A. In *Comprehensive Supramolecular Chemistry*; Gokel, G. W., Ed.; Elsevier: Oxford, U.K., 1996; Vol. *1*, pp 701−732. (b) Miller, S. R.; Gustowski, D. A.; Chen, Z. H.; Gokel, G. W.; Echegoyen, L.; Kaifer, A. E. *Anal. Chem.* **1988**, *60*, 2021−2024.
(28) (a) Amendola, V.; Esteban-Gomez, D.; Fabrizzi, L.; Licchelli, M. *Acc. Chem. Res.* **2006**, *39*, 343−353. (b) Zapata, F.; Caballero, A.; Espinosa, A.; Tárraga, A.; Molina, P. *J. Org. Chem.* **2008**, *73*, 4034−4044.
(29) (a) Kumar, A.; Pandey, P. S. *Org. Lett.* **2008**, *10*, 165−168. (b) Mullen, K. M.; Mercurio, J.; Serpell, C: J.; Beer, P. D. *Angew. Chem., Int. Ed.* **2009**, *48*, 4781−4784. (c) Schulze, B.; Friebe, C.; Hager, M. D.; Günther, W.; Köhn, U.; Jahn, B. O.; Görls, H.; Schubert, U. S. *Org. Lett.* **2010**, *12*, 2710−2713. (d) Ohmatsu, K.; Kiyokawa, M.; Ooi, T. *J. Am. Chem. Soc.* **2011**, *133*, 1307−1309. (e) Chhatra, R. K.; Kumar, A.; Pandey, P. S. *J. Org. Chem.* **2011**, *76*, 9086−9089.
(30) (a) Marder, S. R.; Perry, J. W.; Tiemann, B. G. *Organometallics* **1991**, *10*, 1896−1901. (b) Coe, B. J.; Jones, C. J.; McCleverty, J. A.; Bloor, D.; Cross, G. J. *J. Organomet. Chem.* **1994**, *464*, 225−232. (c) Mller, T. J.; Netz, A.; Ansorge, M. *Organometallics* **1999**, *18*, 5066−5074. (d) Carr, J. D.; Coles, S. J.; Asan, M. B.; Hurthouse, M. B.; Malik, K. M. A.; Tucker, J. H. R. *J. Chem. Soc., Dalton Trans.* **1999**, 57−62.
(31) The association constants were calculated by using the Specfit program (Specfit/32 Global Analysis System, 1999−2004 Spectrum Software Associates (SpecSoft@compuserve.com)). This program was purchased from Bio-logic, SA (www.bio-logic.info) in January 2005.